Electronic Supplementary Material (ESI) for Journal of Materials Chemistry A.

Supporting Information

for

Azine-based polymers with a two-electron redox process as cathode materials for organic batteries

Pascal Acker,[a,b] Martin E. Speer,[a] Jan S. Wössner[a] and Birgit Esser *[a,b,c]

[a]Institute for Organic Chemistry, University of Freiburg, Albertstraße 21, 79104 Freiburg, Germany; besser@oc.uni-freiburg.de; www.esser-lab.uni-freiburg.de

[b]Freiburg Materials Research Center, University of Freiburg, Stefan-Meier-Str. 21, 79104 Freiburg, Germany

[c]Cluster of Excellence livMatS @ FIT – Freiburg Center for Interactive Materials and Bioinspired Technologies, University of Freiburg, Georges-Köhler-Allee 105, 79110 Freiburg, Germany

Table of Contents

1 Experimental procedures

1.1 Materials and methods

Further details can be found in the experimental section of the manuscript.

Air- and moisture-sensitive reactions were performed under an argon atmosphere using standard Schlenk techniques. Commercially available chemicals were used without further purification. Technical grade solvents were distilled prior to use, analytical grade solvents were used as received. Anhydrous solvents were obtained from an MB-SPS 800 System by M. BRAUN and stored over molecular sieves (3 Å).

NMR spectra were recorded at room temperature on a *Bruker Avance III HD 500*, *Bruker Avance Neo 400*, *Bruker Avance II 400* or *Bruker Avance III HD 300* spectrometer. Chemical shifts are reported in parts per million (ppm, δ scale). The ^{1}H and ^{13}C spectra were calibrated against the residual proton and natural abundance ^{13}C resonances of $CDCl_3$ (^{1}H: 7.26 ppm, ^{13}C: 77.16 ppm), DMSO-d_6 (^{1}H: 2.50 ppm, ^{13}C: 39.5 ppm), CD_3CN (^{1}H: 1.94 ppm, ^{13}C: 1.3 ppm), CD_3OD (^{1}H: 3.31 ppm, ^{13}C: 49.0 ppm) or D_2O (^{1}H: 4.79 ppm). The following abbreviations were used: s = singlet, d = duplet, t = triplet, m = multiplet, br = broad. The coupling constants (*J*) are indicated in Hertz (Hz).

HR-MS spectra were measured on a THERMO FISHER SCIENTIFIC Exactive mass spectrometer with an orbitrap analyser with atmospheric-pressure ionization (APCI) or electrospray ionization (ESI) as ionization methods.

MALDI-ToF spectra were measured on an autoflex II TOF/TOF spectrometer from BRUKER.

For **TGA** a *STA 409* or a *STA 449* F5 by NETZSCH and for **DSC** a NETZSCH *DSC 204 F1 Phoenix* were used.

Spectroelectrochemical measurements were measured with an Interface 1000E potentiostat by GAMRY coupled with a SEC 2000 spectrometer by ALS. A platinum net as working electrode, a platinum rod as counter electrode and an $Ag/AgNO_3$ electrode (a silver wire in a chamber filled with 0.1 M $AgNO_3$ and 0.1 M *n*-Bu_4NPF_6) were used.

Cyclic voltammetry in solution was performed inside of a glovebox using a Metrohm Autolab PGSTAT 128N. As working electrode, a glassy carbon disc electrode (2 mm diameters) was used. A platinum rod served as counter electrode, and as reference electrode a $Ag/AgNO_3$ electrode containing a silver wire immersed in an inner chamber filled with 0.1 M $AgNO_3$ in CH_3CN and 0.1 M $^{n}Bu_4NPF_6$ in DMF in the outer chamber were used. For the internal reference, the ferrocene/ferrocenium (Fc/Fc^{+}) redox couple was used.

Electrochemical measurements in cells were conducted on a *MPG-2* potentiostat from BIOLOGIC SCIENCE INSTRUMENTS.

ATR-FT-IR-spectroscopy was carried out with a Nicolet 14iS10 FT-IR spectrometer from THERMO SCIENTIFIC equipped with a diamond ATR-unit.

Raman spectroscopy was conducted on a BRUKER S*enterra II* Raman microscope with ZEISS-optic. Optical micrographs were taken with 20× magnification and Raman spectra were recorded with a 785 nm laser (1 mW) and 100 scans per spectra with a resolution of 4 cm^{-1}.

Scanning Electron Microscopy: High resolution scanning electron microscopy (SEM) measurements were conducted on a THERMO FISHER SCIENTIFIC *Scios 2 DualBeam* with an AMETEK EDAX *Octane Elite EDS System* for EDX mapping.

DFT-calculations: see respective chapter for further details.

1.1 Elemental analysis of polymer P3

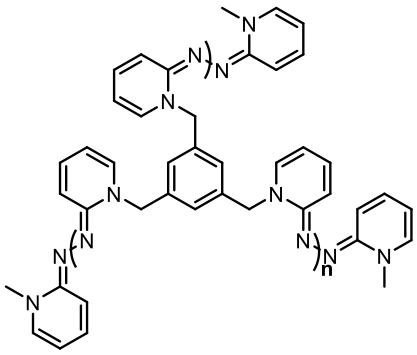

Table S 1: Found element contents in elemental analysis of polymer **P3**.

Exper. Number	C	H	N
1	71.42%	5.88%	21.30%
2	71.05%	5.95%	21.20%

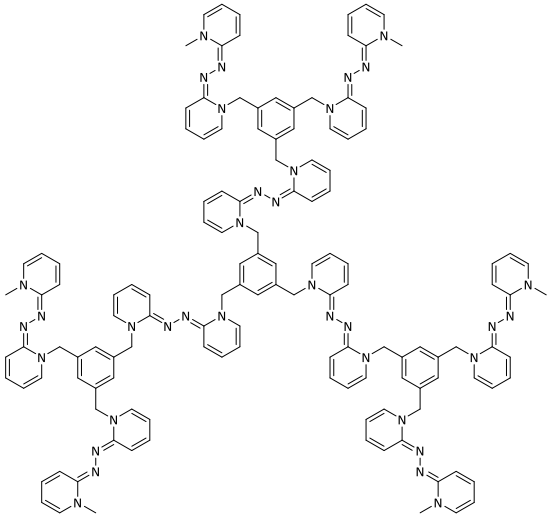

Chemical Formula: $C_{132}H_{126}N_{36}$
Elemental Analysis: C, 71.52; H, 5.73; N, 22.75

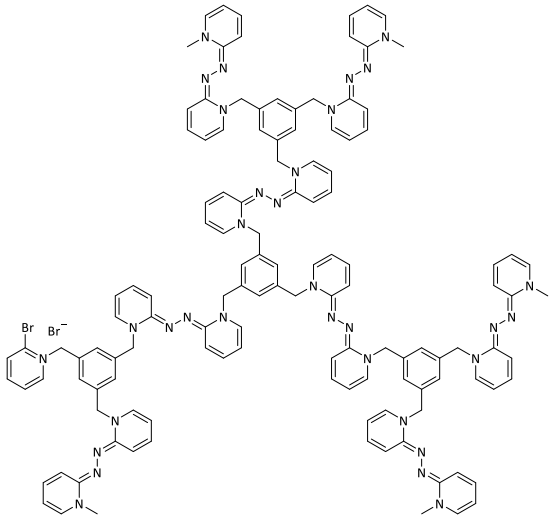

Chemical Formula: $C_{126}H_{119}Br_2N_{33}^{+}$
Elemental Analysis: C, 67.10; H, 5.32; Br, 7.09; N, 20.49

Figure S 1: Left: Most probable structure; right: Structure with defect, carbon and nitrogen contents are heavily decreased; higher molecular weight leads to increase in C and decrease in H and N. The most probable structure is depicted above, probably some structures have defects.

2 NMR spectra

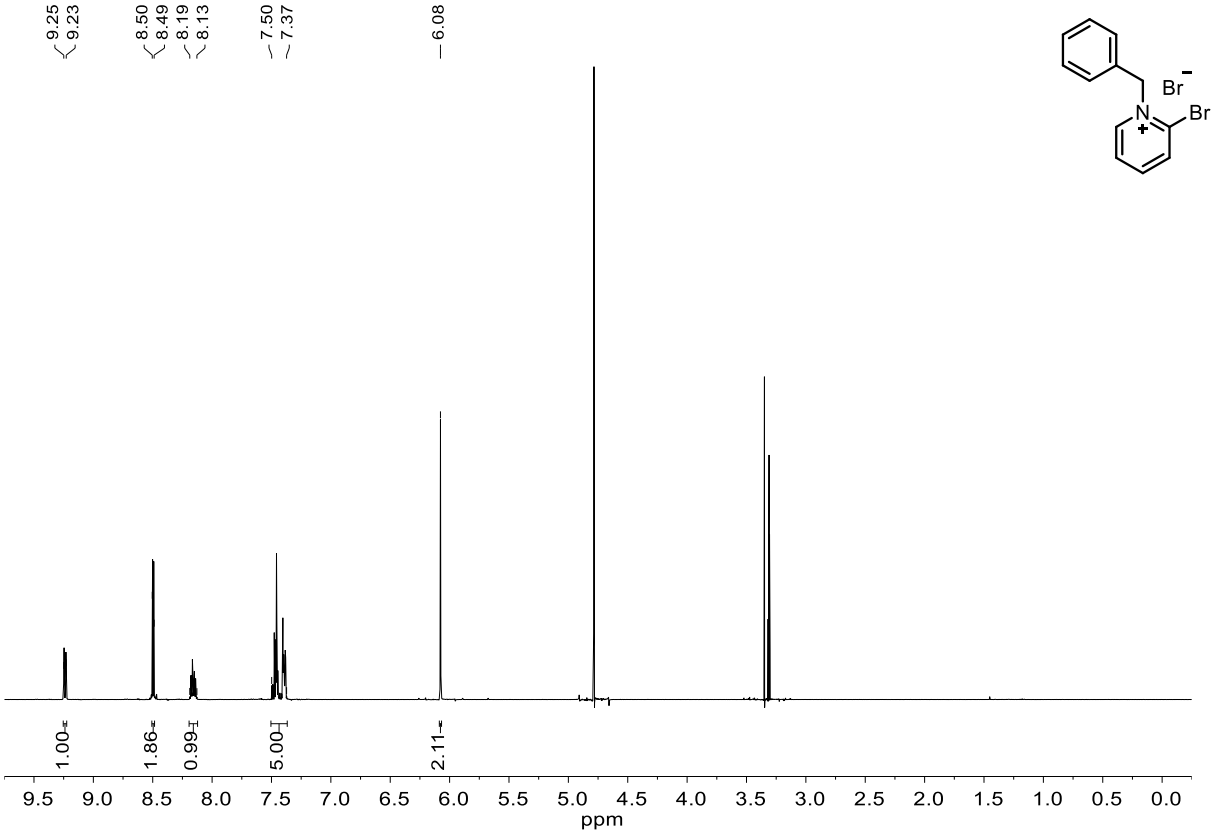

Figure S 2: ^{1}H NMR spectrum of **9** (CD_3OD, 400 MHz).

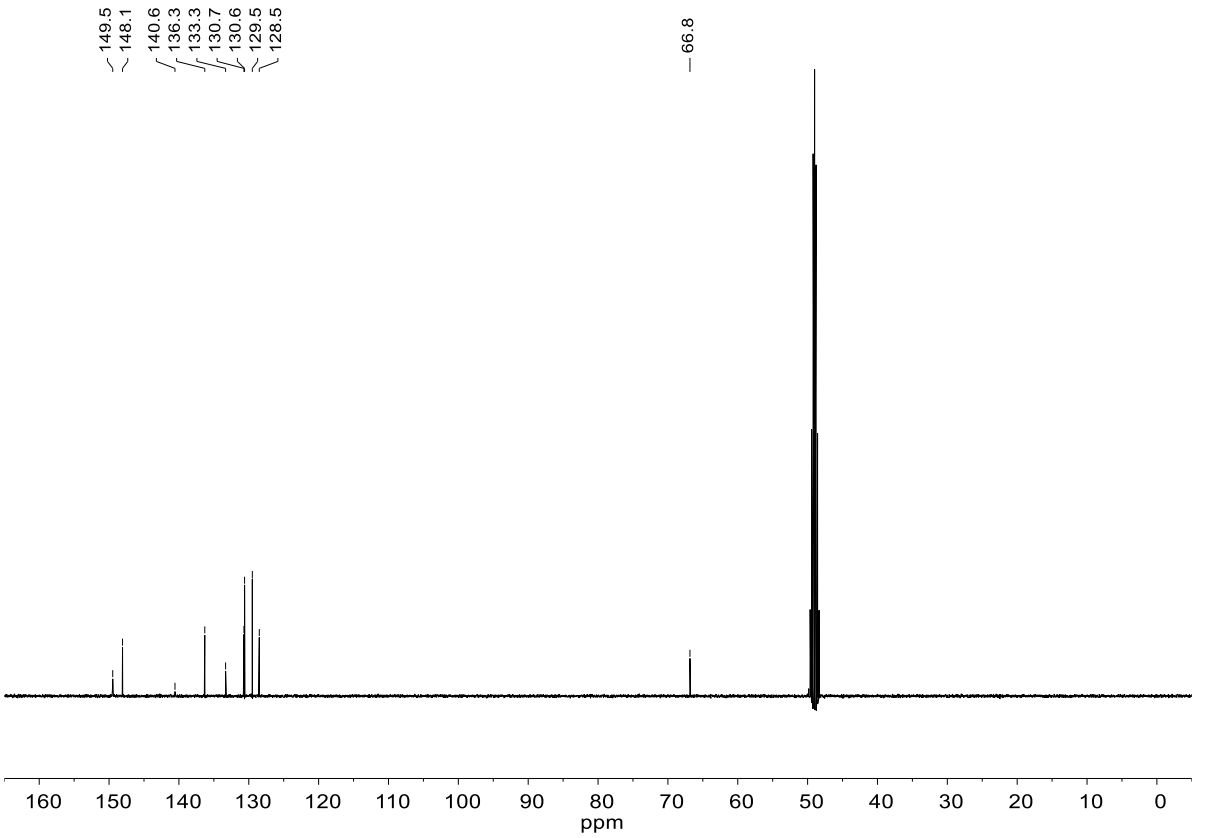

Figure S 3: ^{13}C NMR spectrum of **9** (CD_3OD, 101 MHz).

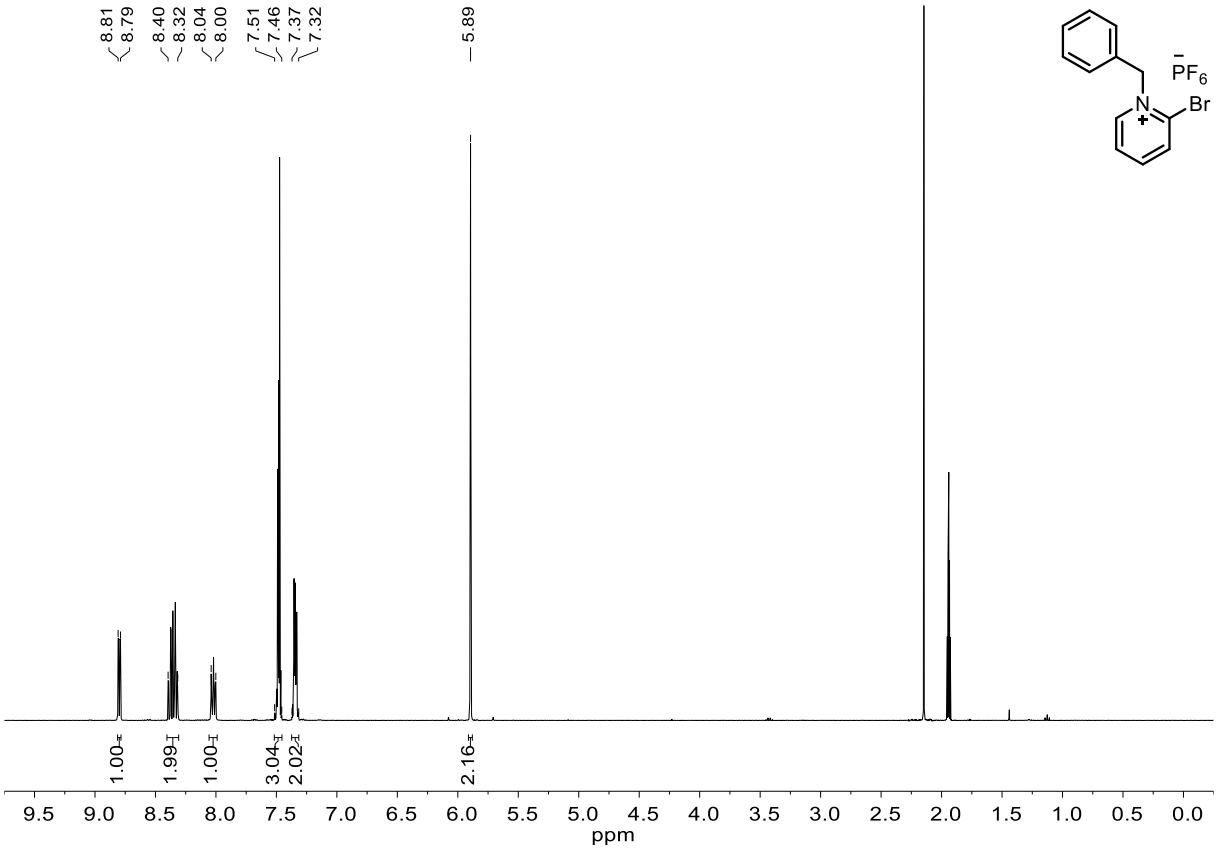

Figure S 4: ^{1}H NMR spectrum of **4** (CD_3CN, 400 MHz).

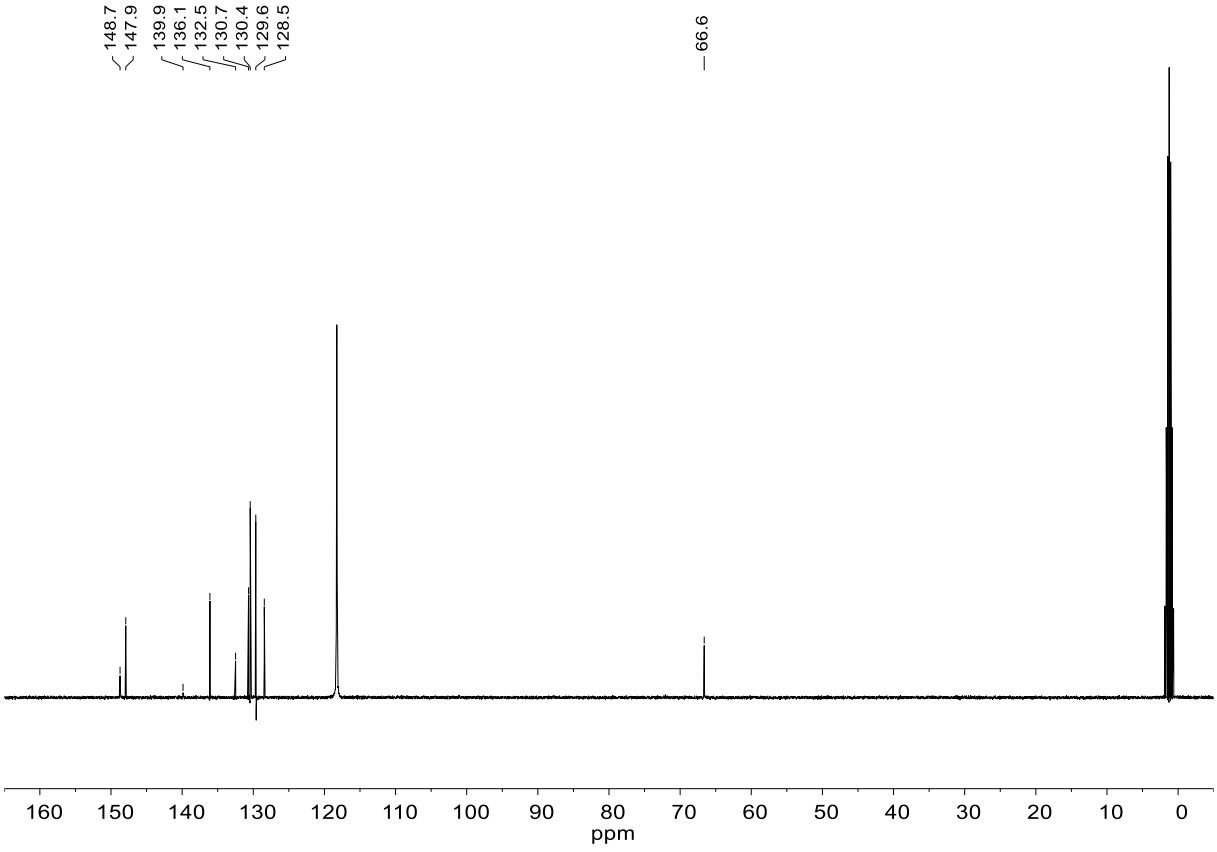

Figure S 5: ^{13}C NMR spectrum of **4** (CD_3CN, 101 MHz).

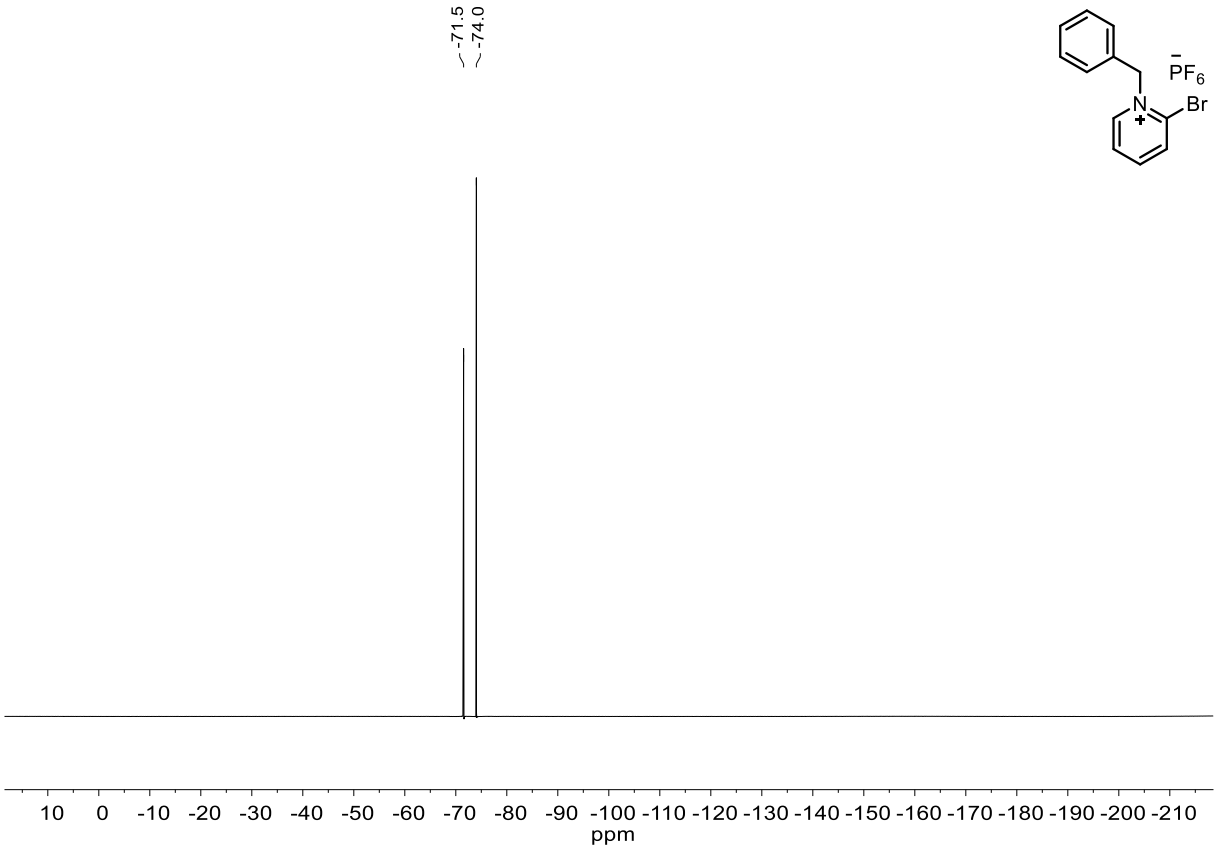

Figure S 6: ^{19}F NMR spectrum of **4** (CD_3CN, 282 MHz).

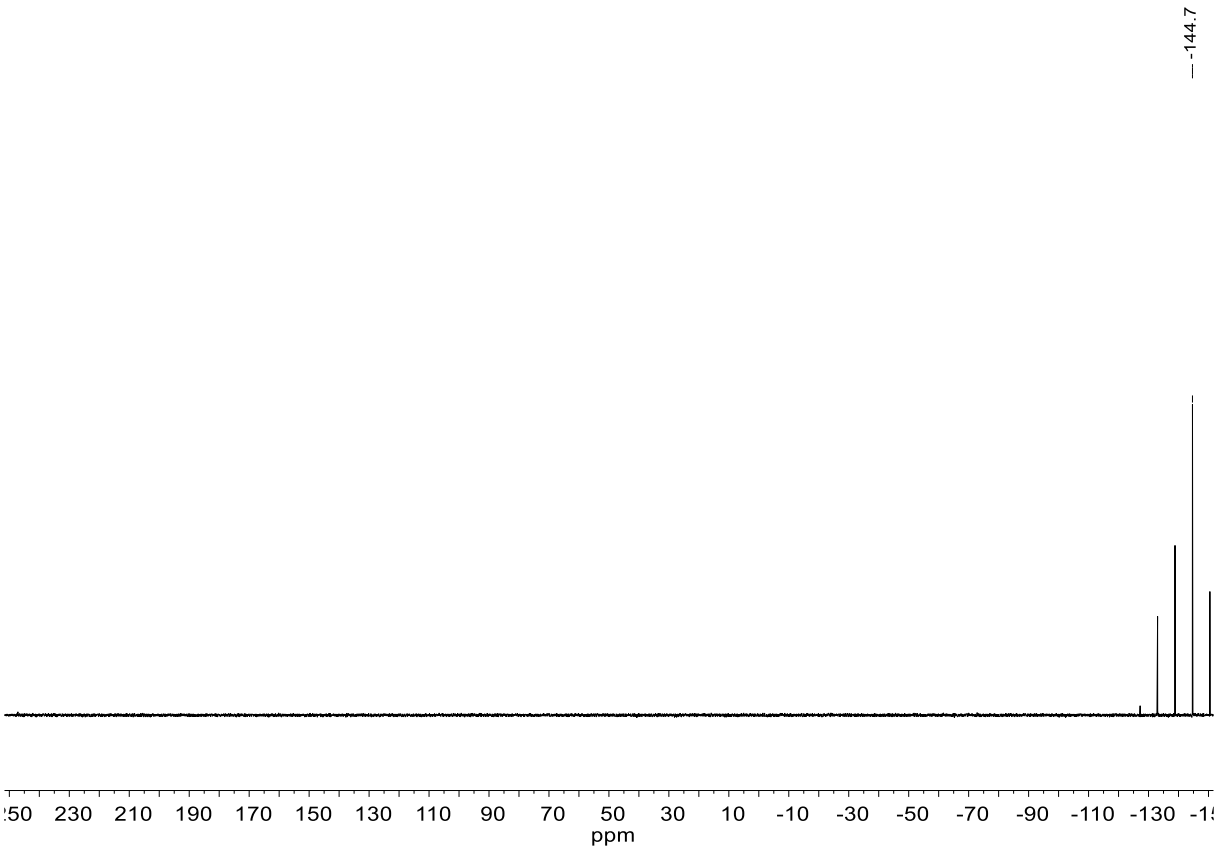

Figure S 7: ^{31}P NMR spectrum of **4** (CD_3CN, 121 MHz).

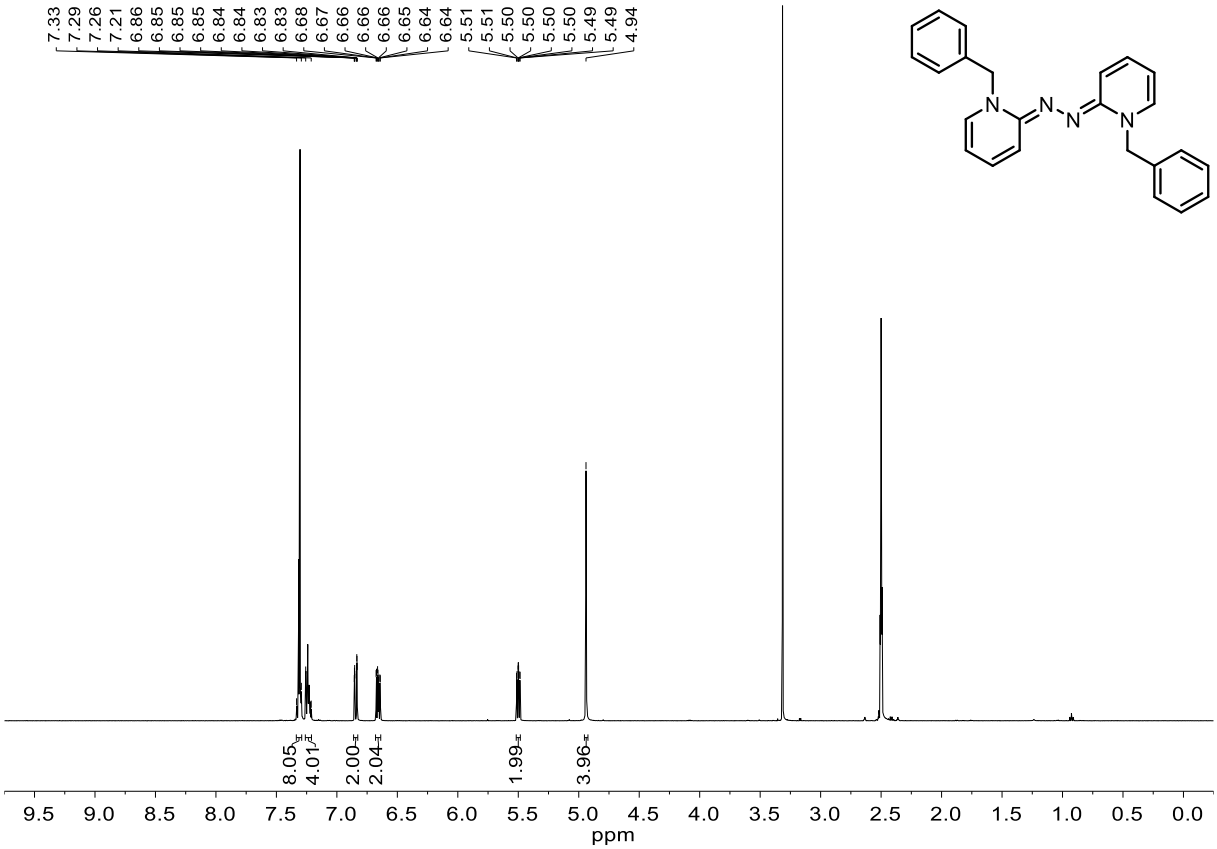

Figure S 8: ^{1}H NMR spectrum of **2** (DMSO-d_6, 500 MHz).

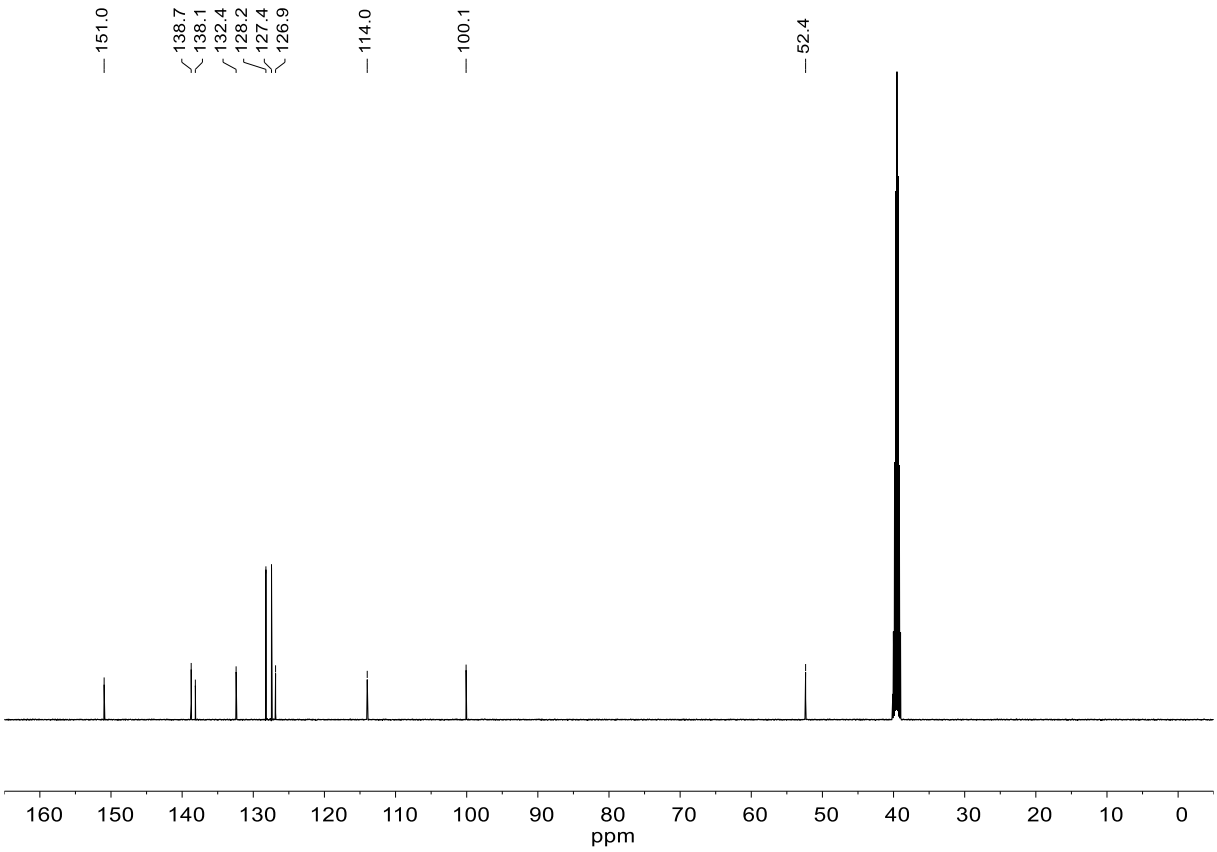

Figure S 9: ^{13}C NMR spectrum of **2** (DMSO-d_6, 126 MHz).

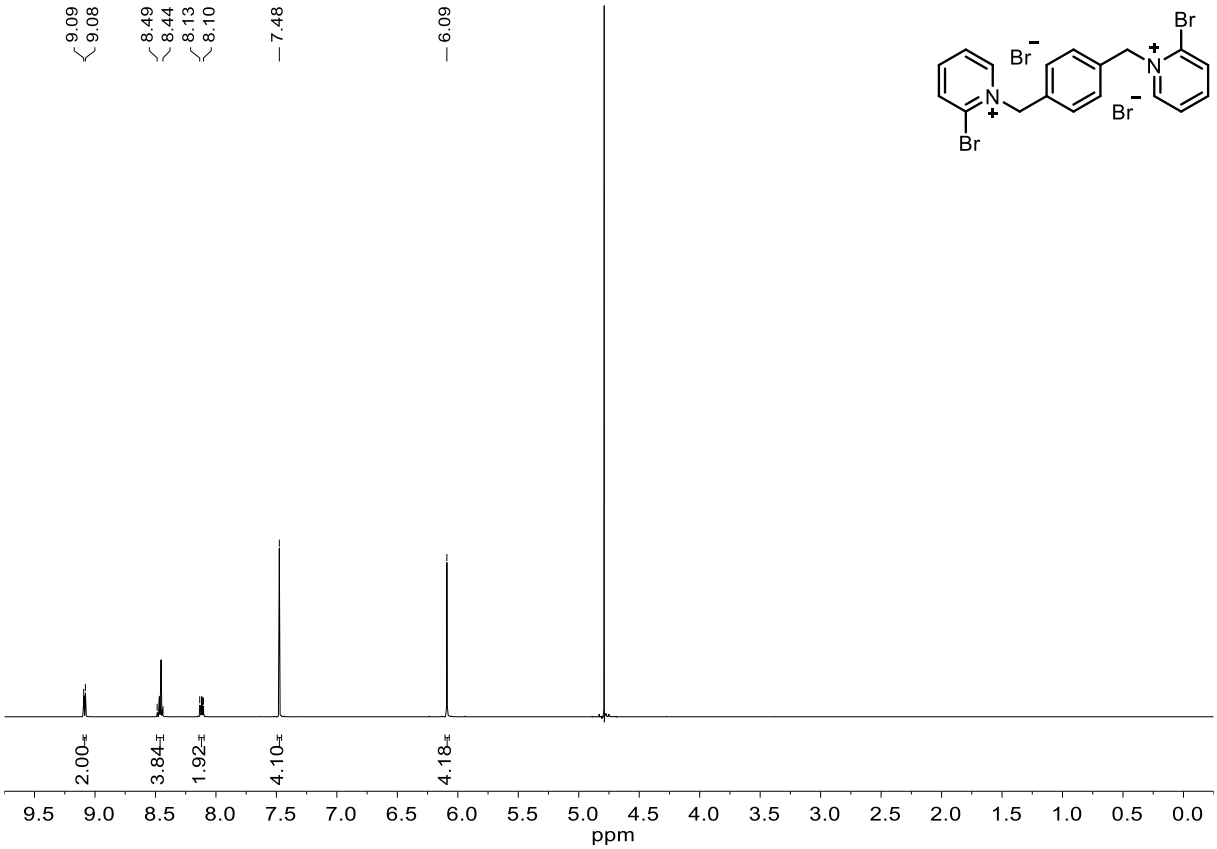

Figure S 10: ^{1}H NMR spectrum of **6** (D_2O, 500 MHz).

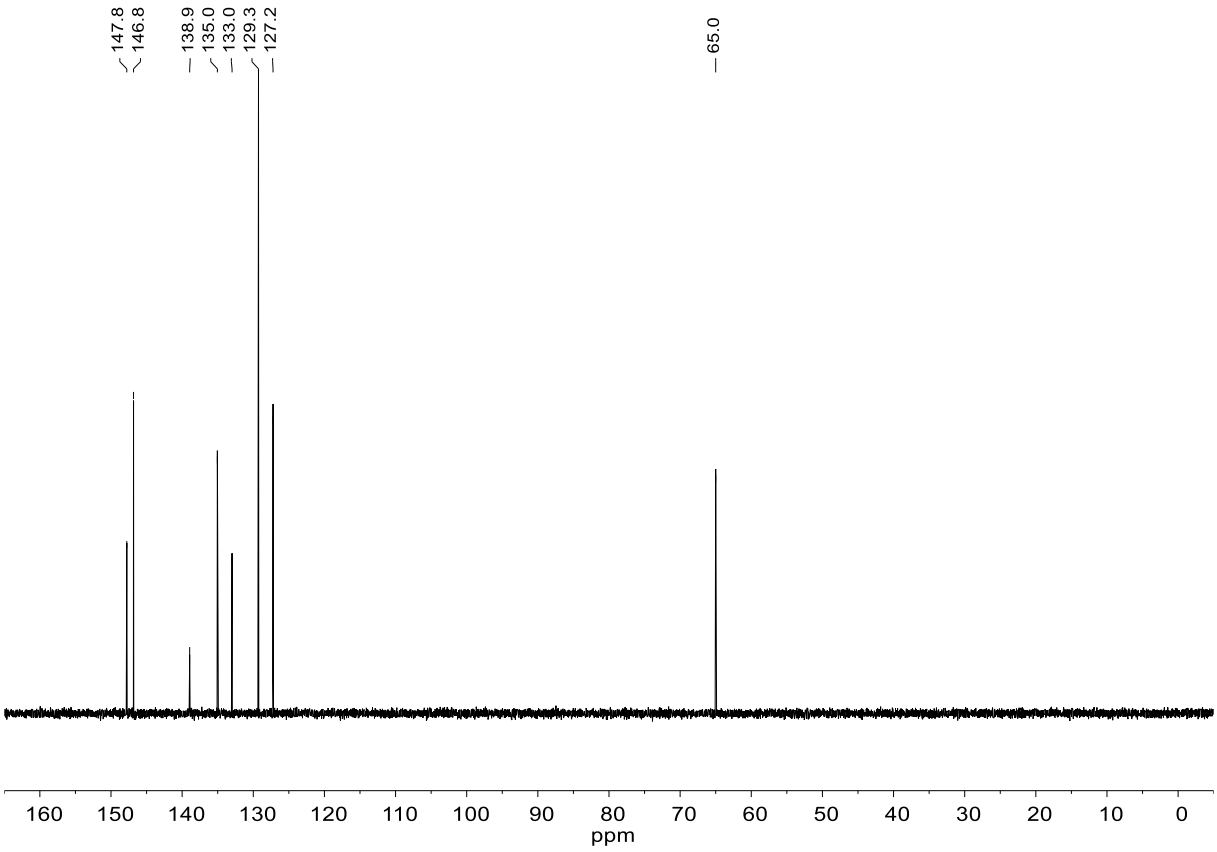

Figure S 11: ^{13}C NMR spectrum of **6** (D_2O, 126 MHz).

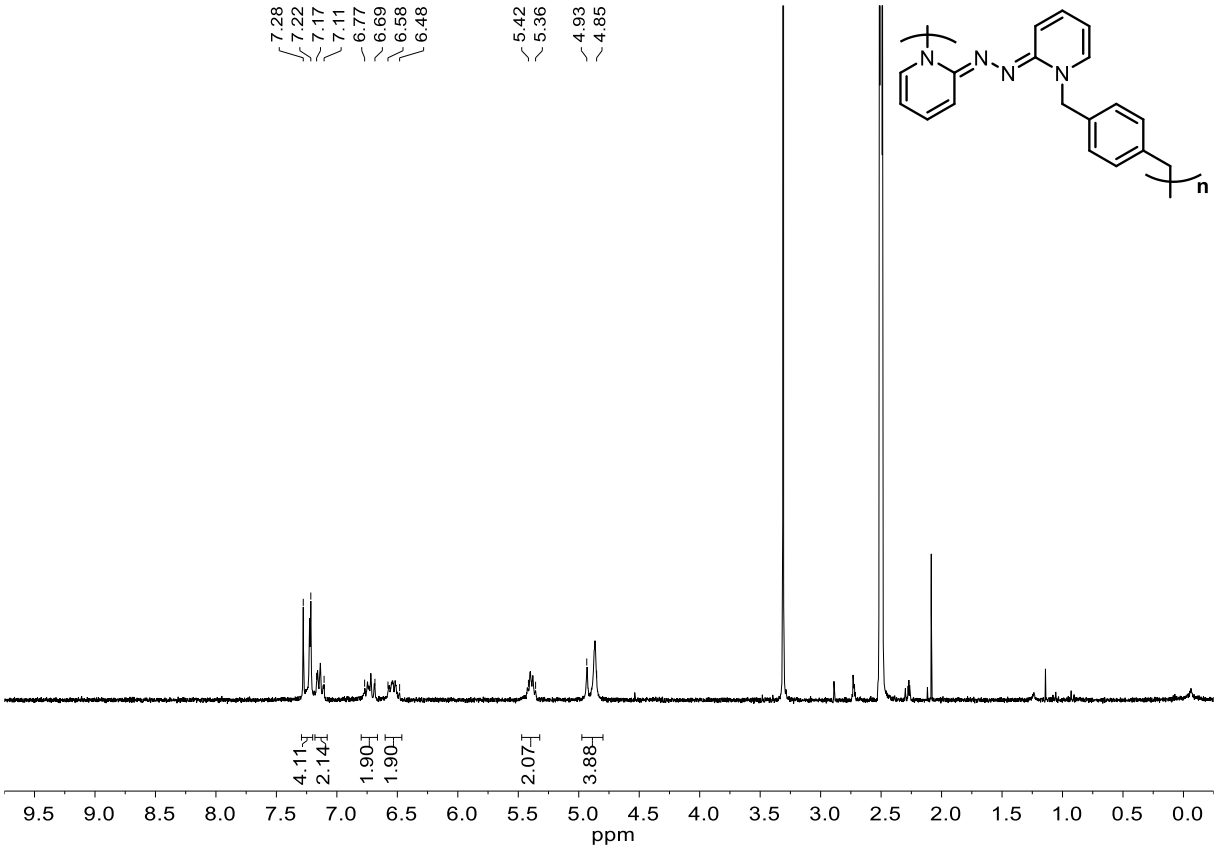

Figure S 12: ^{1}H NMR spectrum of **P1** (DMSO-d_6, 300 MHz).

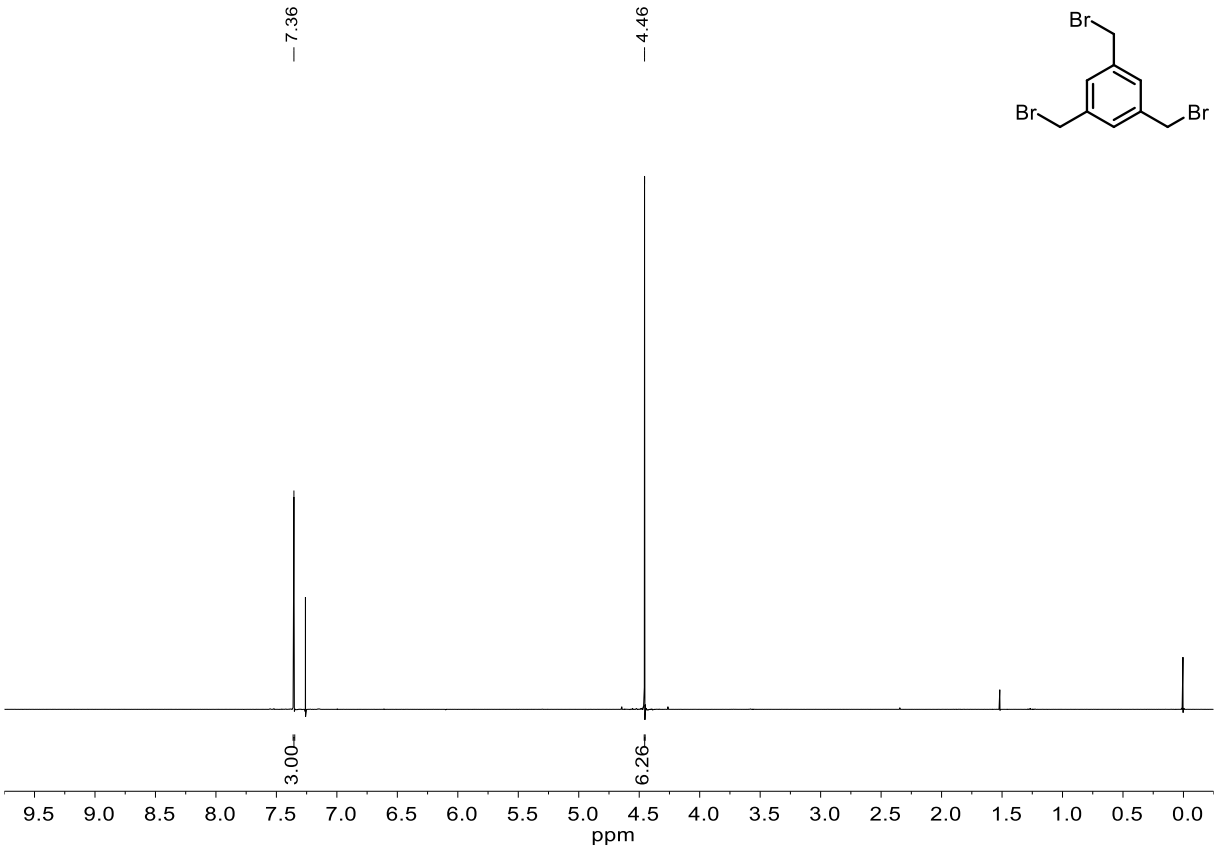

Figure S 13: ^{1}H NMR spectrum of **7** ($CDCl_3$, 400 MHz).

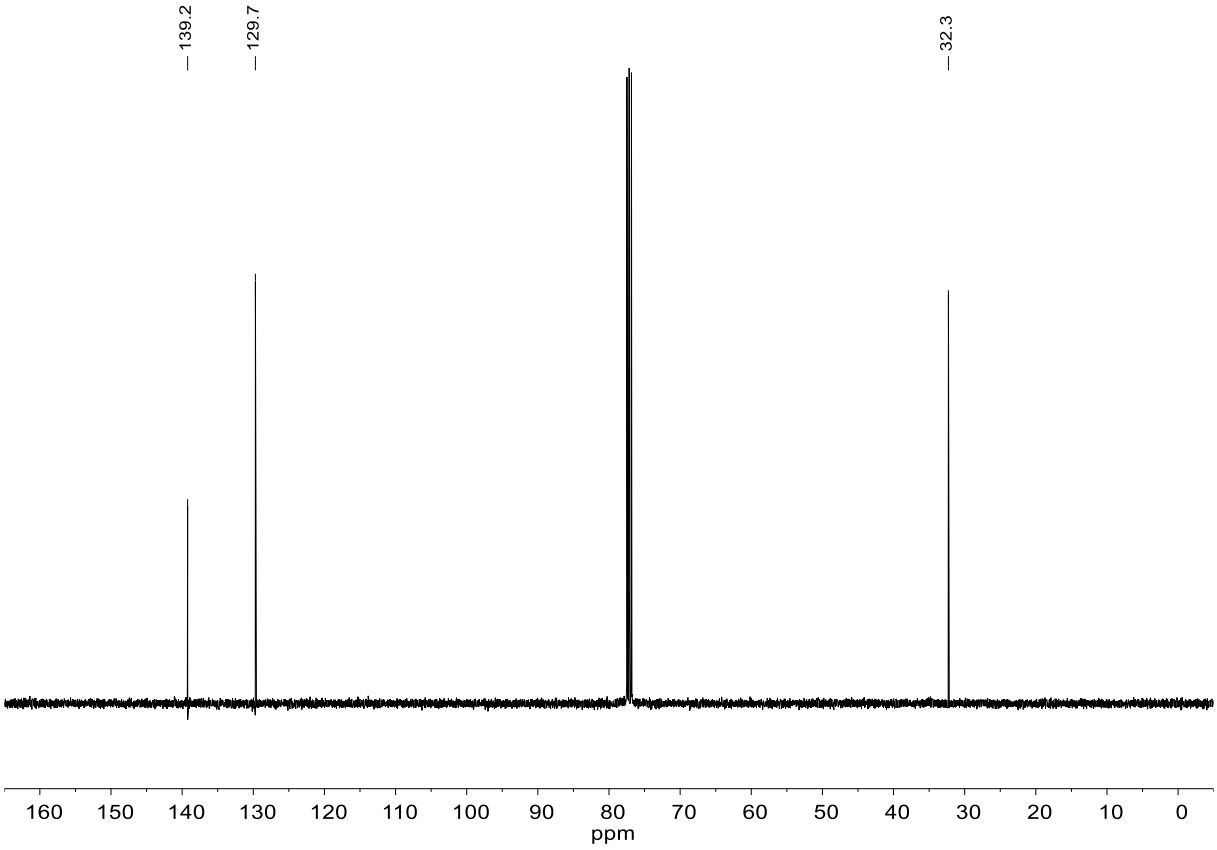

Figure S 14: ^{13}C NMR spectrum of **7** ($CDCl_3$, 101 MHz).

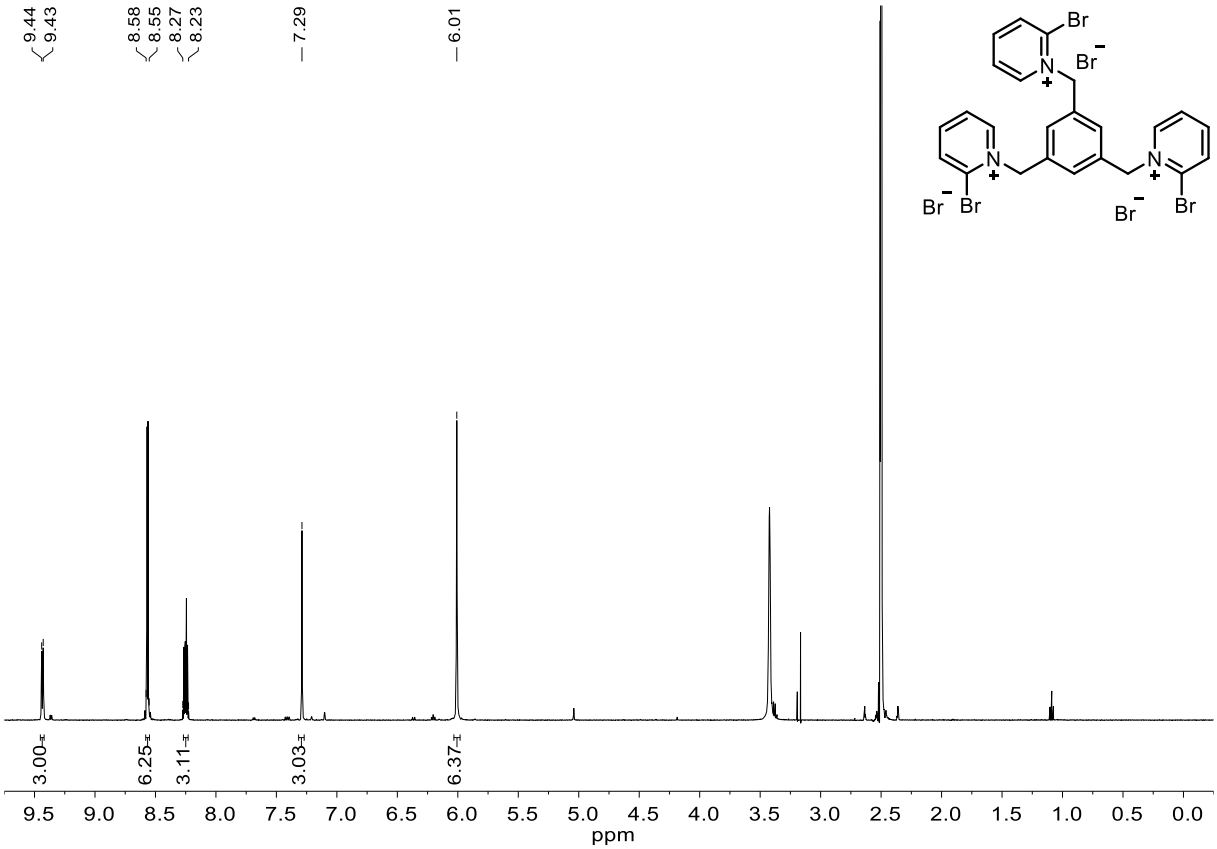

Figure S 15: ^{1}H NMR spectrum of **8** (DMSO-d_6, 500 MHz).

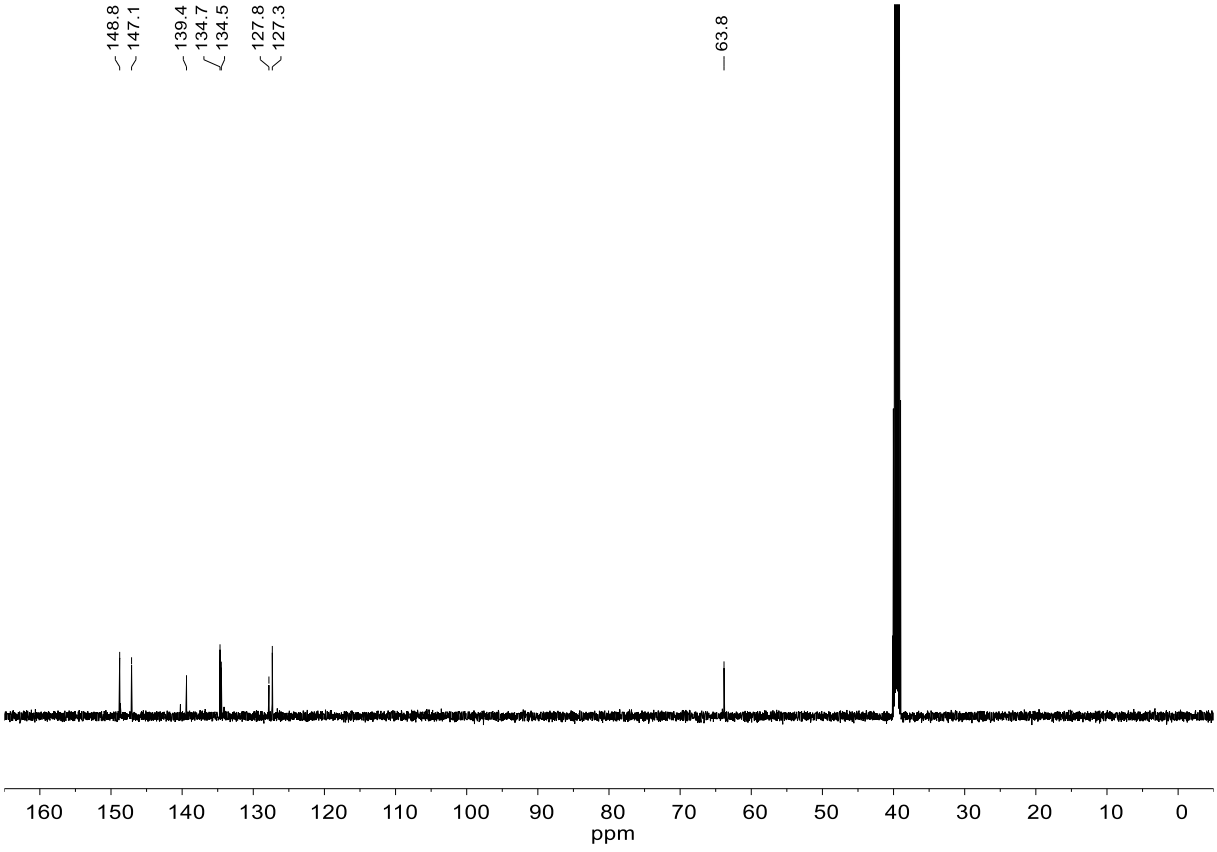

Figure S 16: ^{13}C NMR spectrum of **8** (DMSO-d_6, 126 MHz).

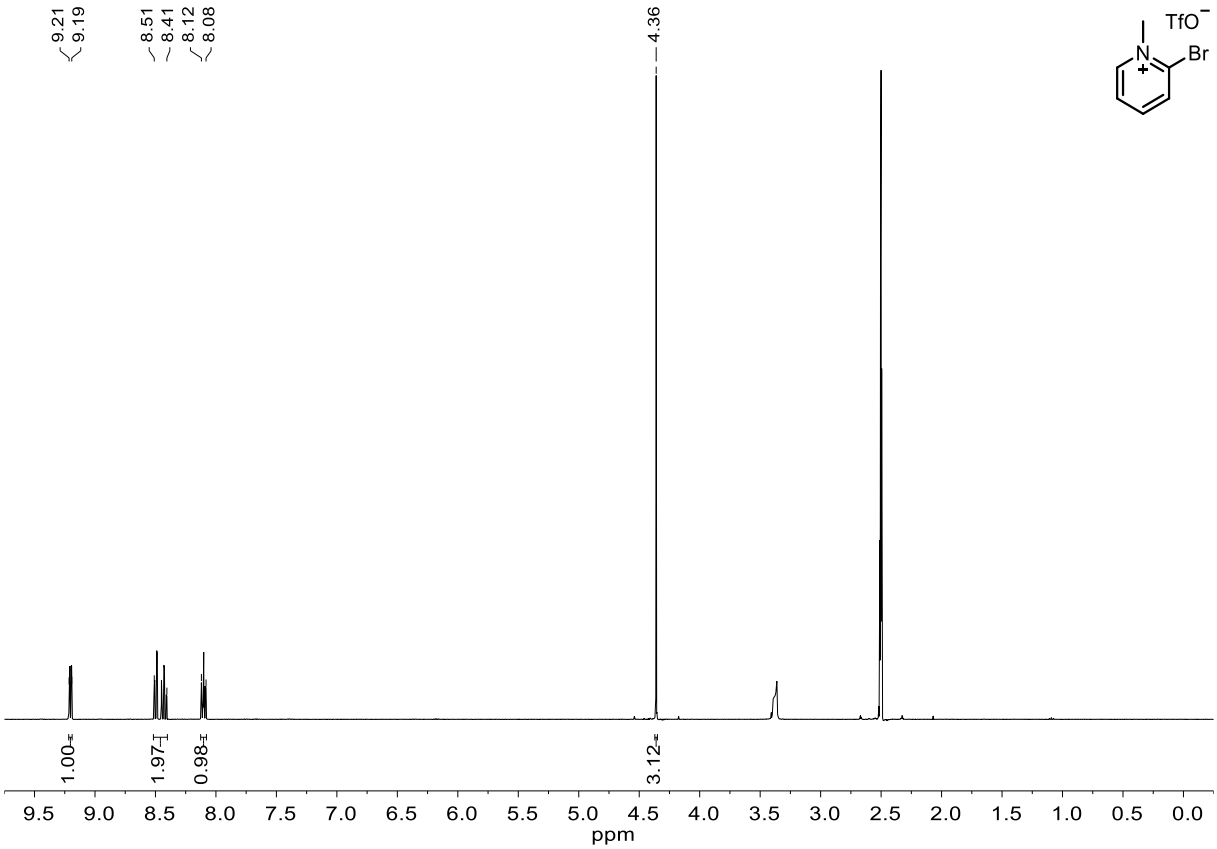

Figure S 17: ^{1}H NMR spectrum of **10** (DMSO-d_6, 400 MHz).

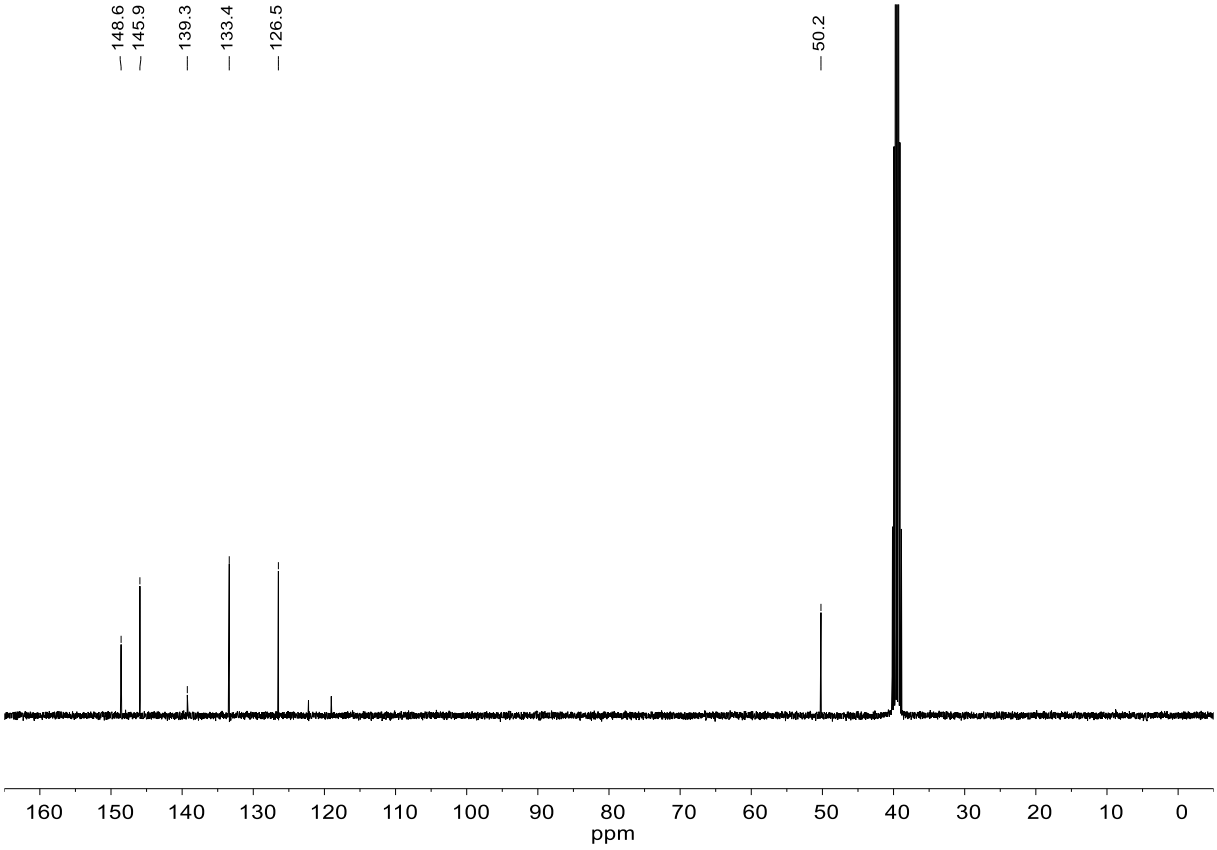

Figure S 18: ^{13}C NMR spectrum of **10** (DMSO-d_6, 100 MHz).

3 Electrochemical investigations

3.1 Investigations of P1-based composite electrodes

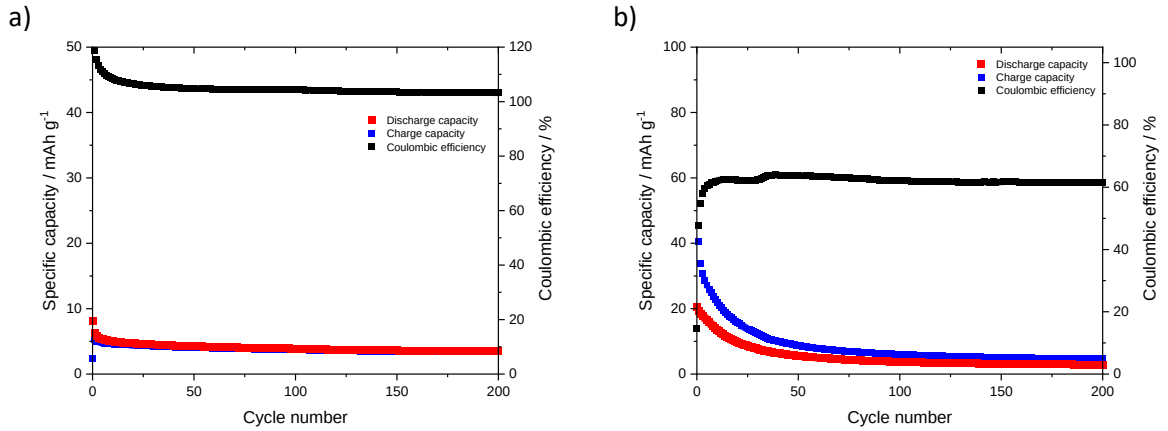

Figure S 19: Constant current cycling of a **P1**-based composite electrodes with different electrolytes, Li metal as counter and reference electrode at 1C rate; a) 1 M $LiPF_6$ in EC/DMC: 1/1; b) 1 M $LiClO_4$ in DOL.

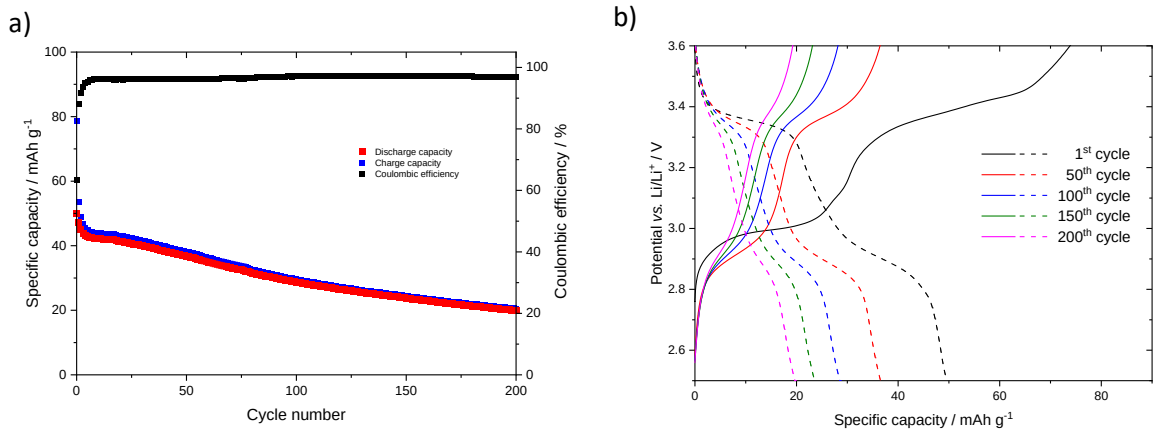

Figure S 20: Constant current cycling of a **P1**-based composite electrode with 2 M $LiClO_4$ in DOL/DME: 1/1; a) Specific capacity vs. cycle number; b) charge/discharge curves of selected cycles.

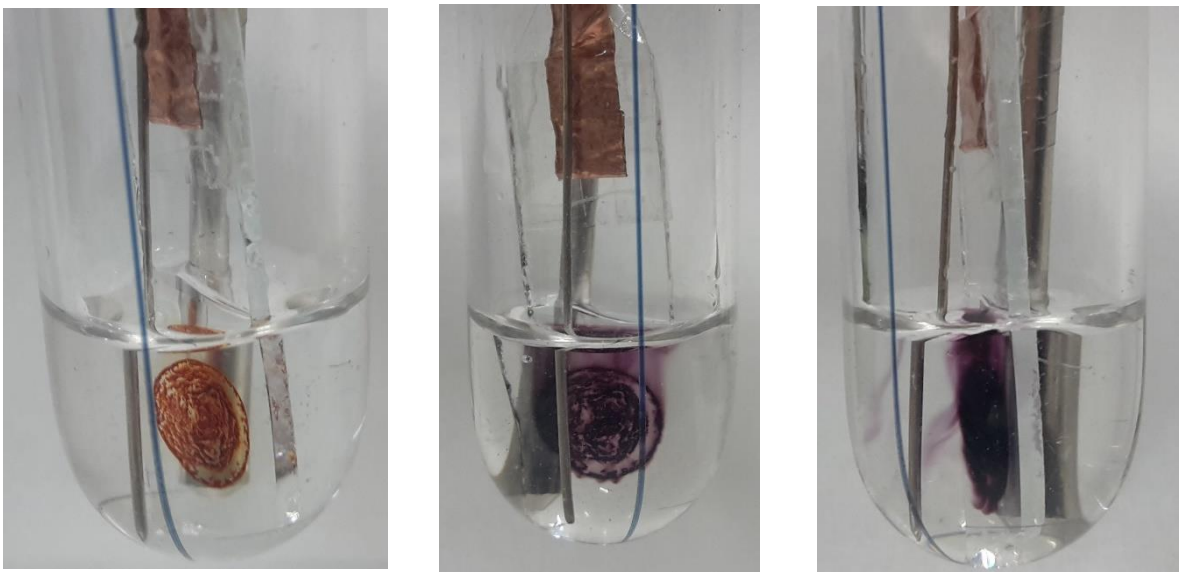

Figure S 21: Solubility test of a **P1**-polymer film in electrolyte solution (1 M $LiPF_6$ in EC/DMC: 1/1), the dissolution is clearly visible; left: neutral state; middle and right: oxidized state.

3.2 Investigations of P2-based composite electrodes

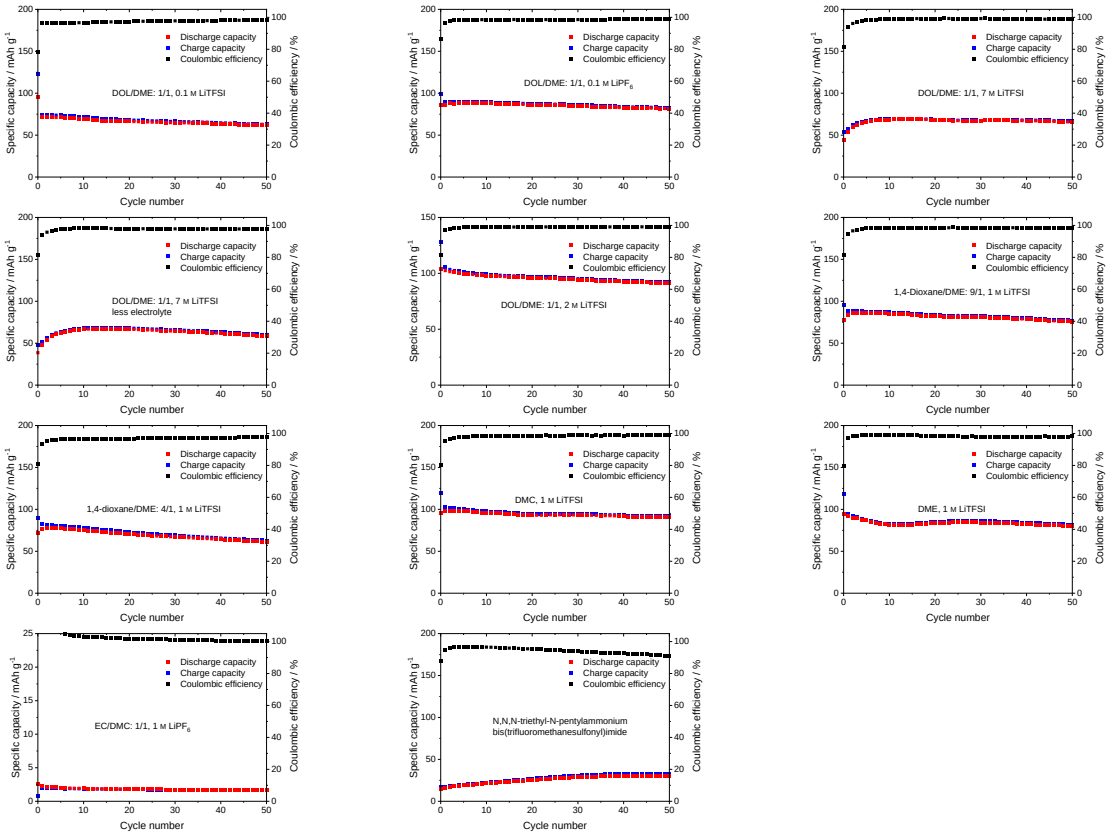

Figure S 22: Constant current cycling of **P2**-based composite electrodes using different electrolytes with Li metal as counter and reference electrode at 1C-rate.

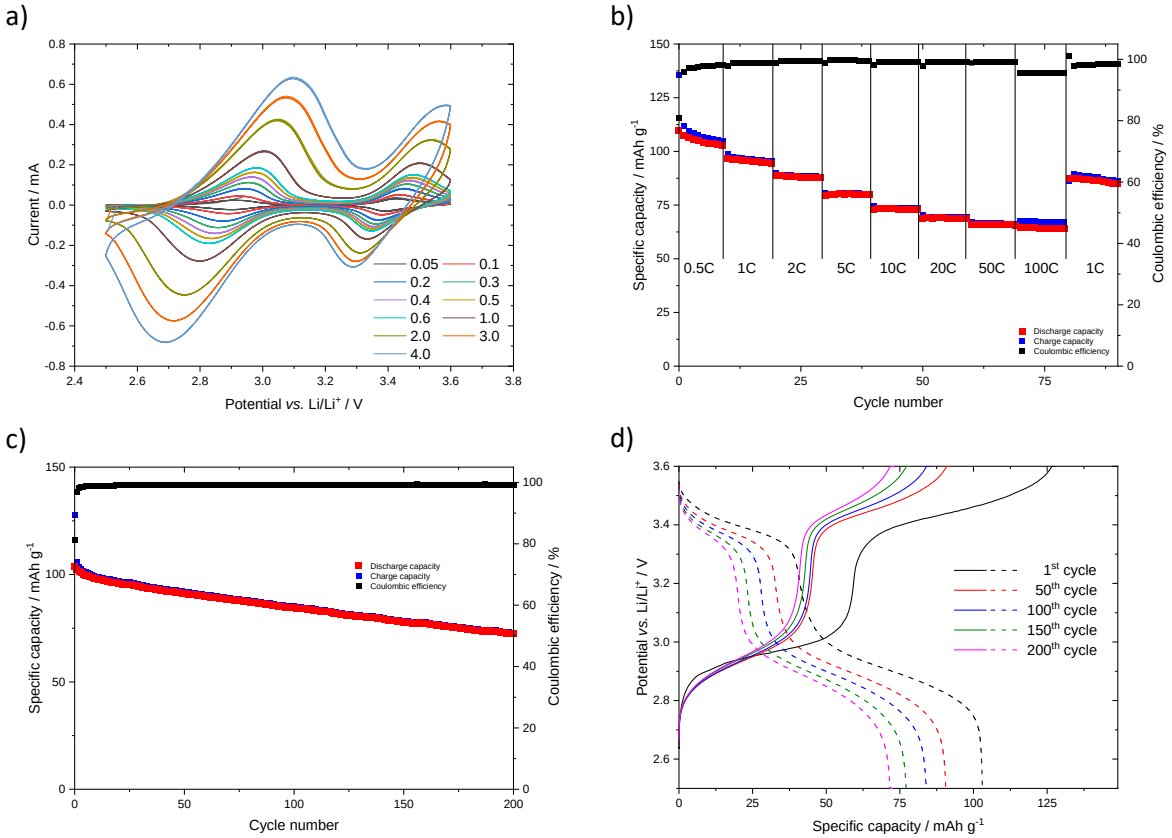

Figure S 23: Electrochemical investigations of **P2**-based composite electrodes with optimized electrolyte (2 M LiTFSI in DOL/DME: 1/1), Li metal as counter and reference electrode; a) cyclic voltammograms at different scan rates in mV s^{-1}; b) rate capability test in the voltage range of 2.5–3.6 V; c) constant current cycling in the voltage range of 2.5–3.6 V; d) charge/discharge curves of selected cycles.

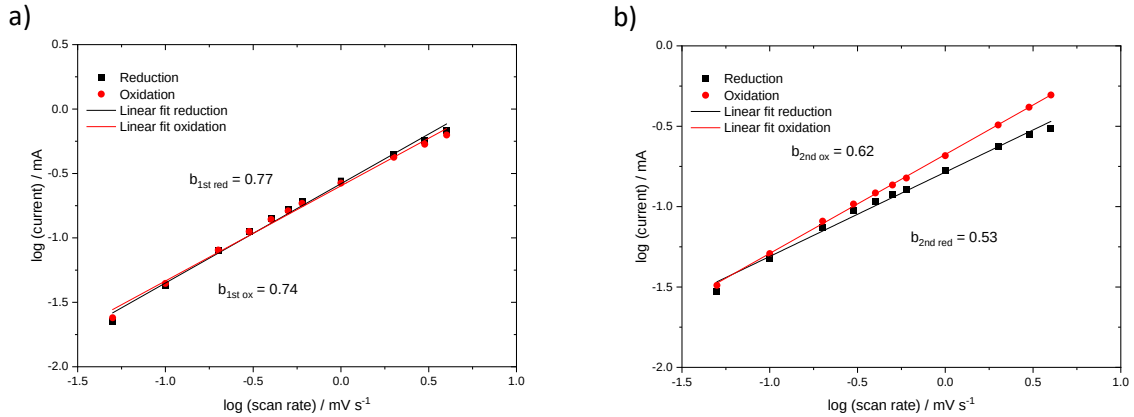

Figure S 24: Investigation of the faradaic and capacitive nature of the a) first and b) second redox process in **P2**-based composite electrodes.

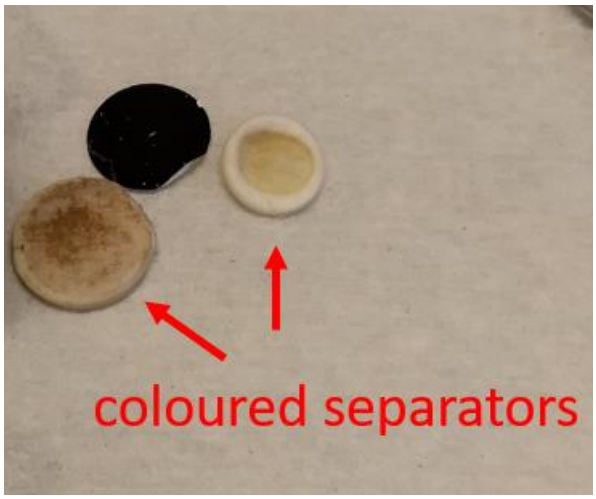

Figure S 25: Post mortem analysis of a **P2**-based cycled cell; separators are heavily coloured.

3.3 Investigations of P3-based composite electrodes

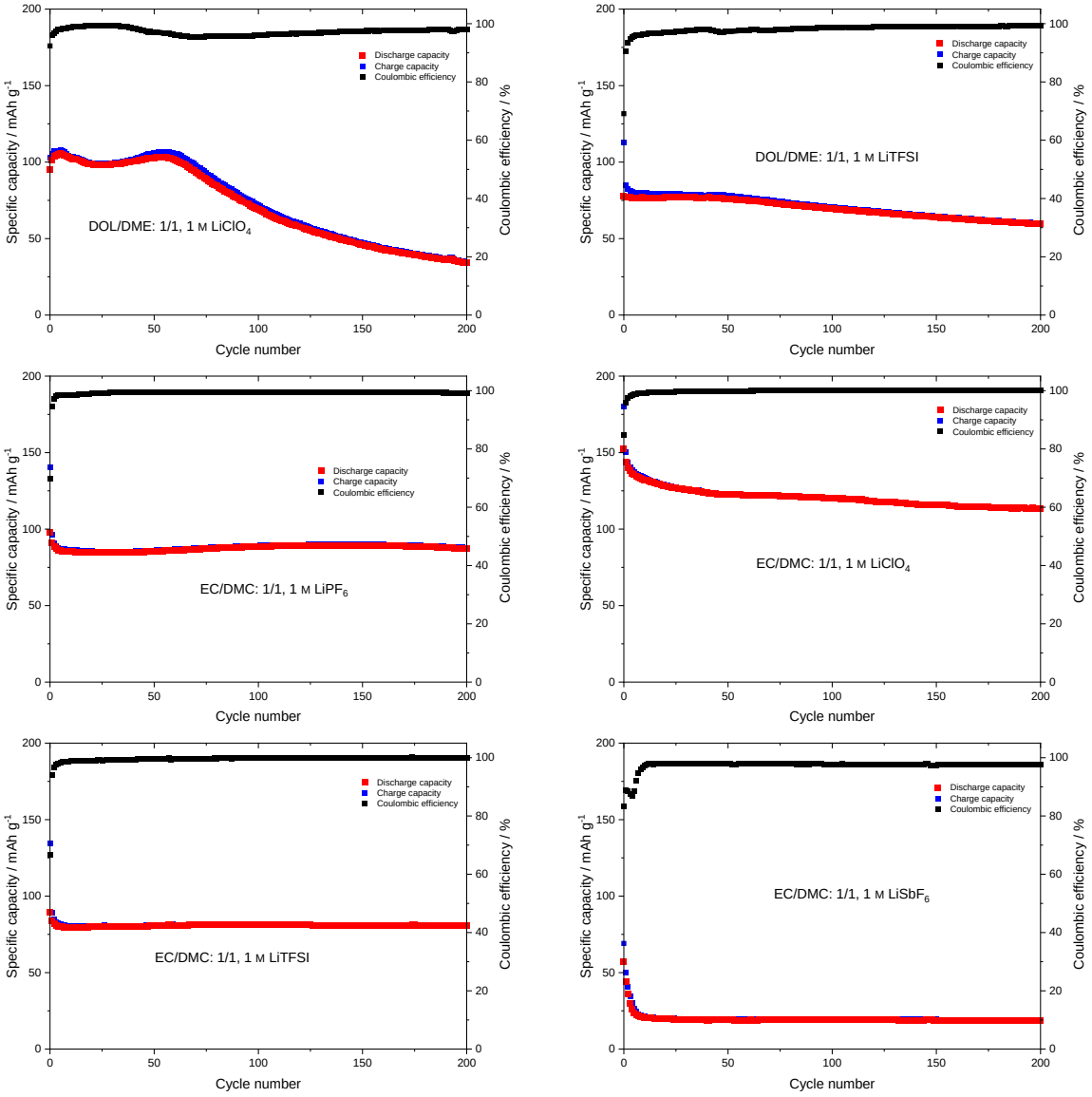

Figure S 26: Constant current cycling of **P3**-based composite electrodes using different electrolytes with Li metal as counter and reference electrode at 1C-rate.

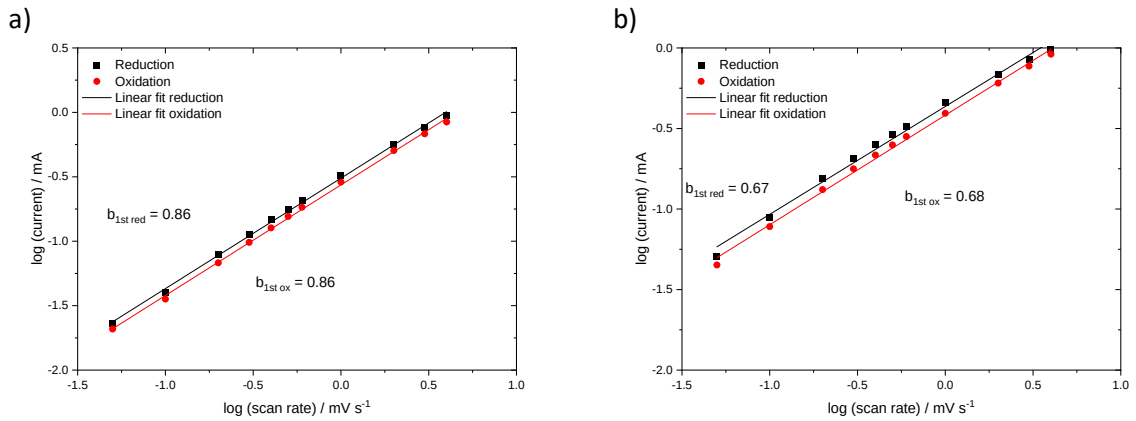

Figure S 27: Investigation of the faradaic and capacitive nature of the a) first and b) second redox process in a **P3**-based composite electrode.

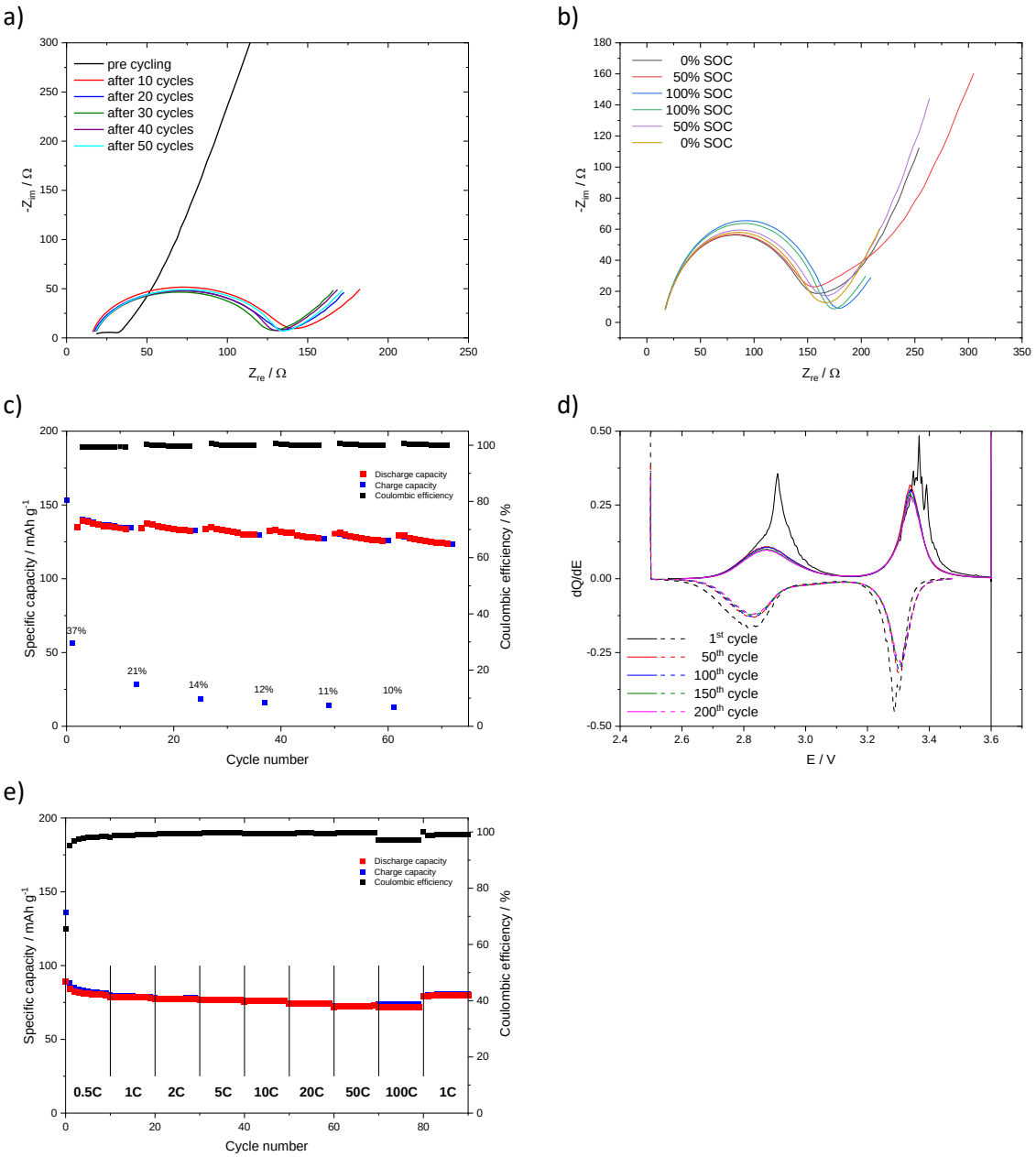

Figure S 28: Electrochemical performance of **P3**-based composite electrodes: a) EIS measurements after several cycles in constant current mode; b) EIS measurements in different state-of-charge (SOC) conditions; c) self-discharge test, 10 cycles constant current cycling at 1C rate, followed by a 72 h rest step in the charged state; d) differential capacity plot (data from constant current cycling test at 1C-rate, see Figure 3b and c); e) rate capability test of **P3**-based composite with 1 M $LiPF_6$ in EC/DMC: 1/1 (v/v).

4 IR/Raman spectroscopy

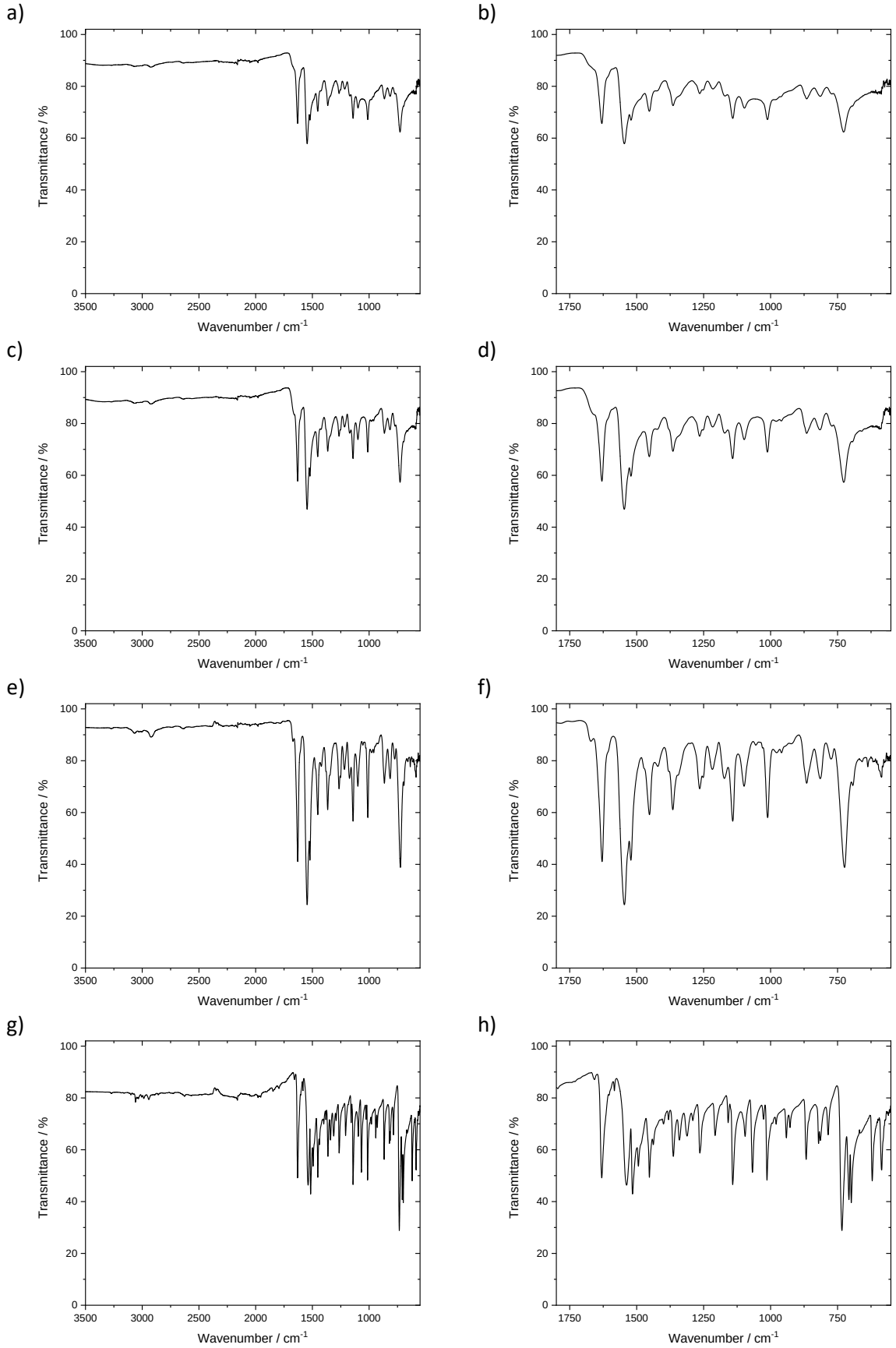

Figure S 29: IR spectra of polymers **P1** (a, b), **P2** (c, d) and **P3** (e, f) and the model compound **2** (g, h).

Table S 2: In infrared spectroscopy observed signals of polymers **P1**, **P2** and **P3** and of the model compound **2**.[1]

Signal	Vibration	P1	P2	P3	2
3067 (vw)	=C-H ar str vib	✓	✓	✓	
3059 (vw)	=C-H ar str vib	×	×	×	✓
2942 (vw)		×	×	×	✓
2925 (vw)		✓	✓	✓	×
1629 (s)	asym C=N-N=C str	✓	✓	✓	✓
1546 (s)	sym.C=N-N=C str	✓	✓	✓	×
1538 (s)	sym.C=N-N=C str	×	×	×	✓
1522 (w)	C=C	✓	✓	✓	×
1516 (w)		×	×	×	✓
1453 (m)		✓	✓	✓	✓
1363 (w)		✓	✓	✓	✓
1264 (w) split bei Poly		✓	✓	✓	✓
1141 (w)		✓	✓	✓	✓
1097 (vw)		✓	✓	✓	✓
1068 (w)		×	×	×	✓
1013 (w)		✓	✓	✓	✓
867 (w)	=C-H out-of-plane def vib	✓	✓	✓	✓
734 (s)	Ar-CH_2, C-H out-of-plane def vib, ring def vib	×	×	×	✓
724 (s)	Ar-CH_2, C-H out-of-plane def vib, ring def vib	✓	✓	✓	×
708 (m)	=C-H out-of-plane deff vib	×	×	×	✓
699 (m)	Ar-CH_2, C-H out-of-plane def vib, ring def vib	×	×	×	✓
621 (m)	Ar-CH_2, C-H out-of-plane def vib, ring def vib	×	×	×	✓
586 (m)		×	×	×	✓
585 (w)		×	×	✓	×

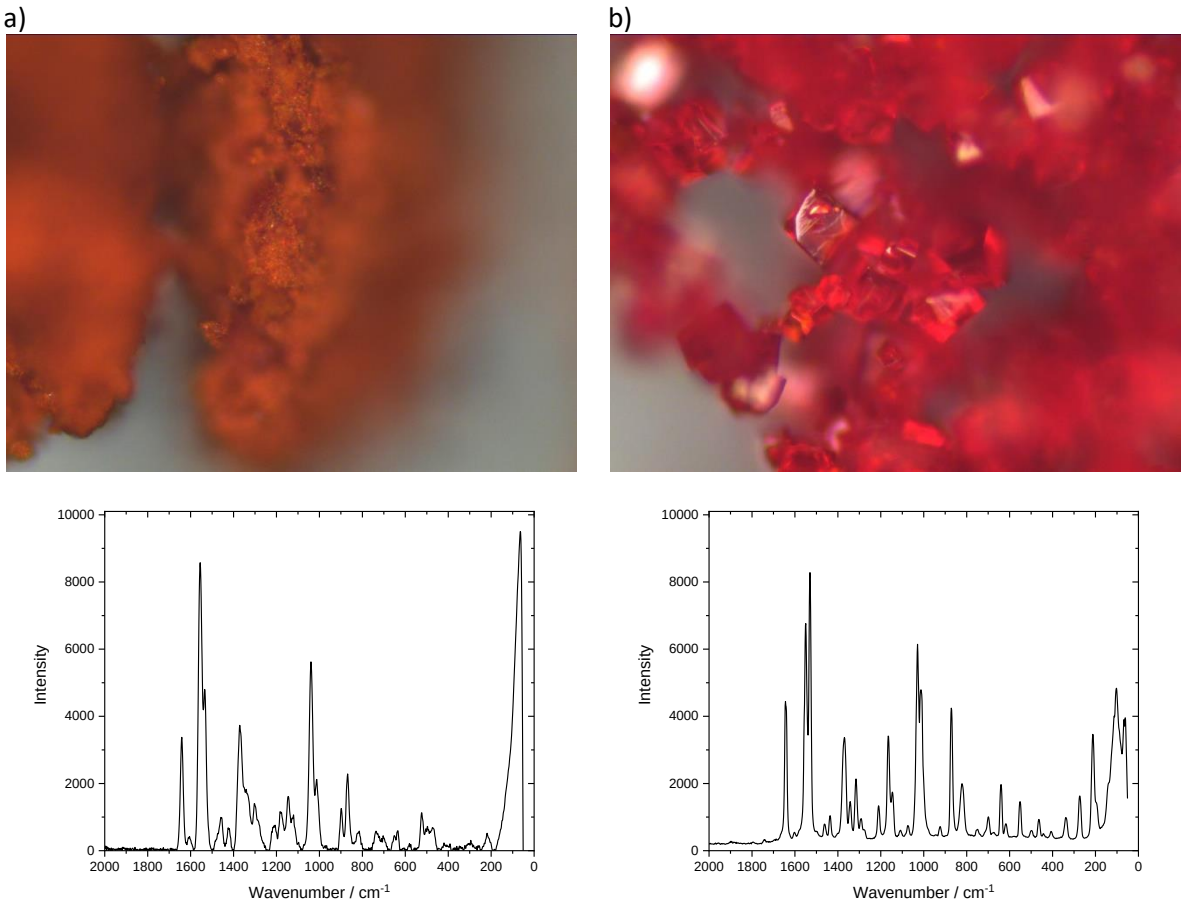

Figure S 30: Optical micrographs (20x magnification) and Raman spectra of polymer **P3** (a) and model compound **2** (b).

5 MALDI spectrometry

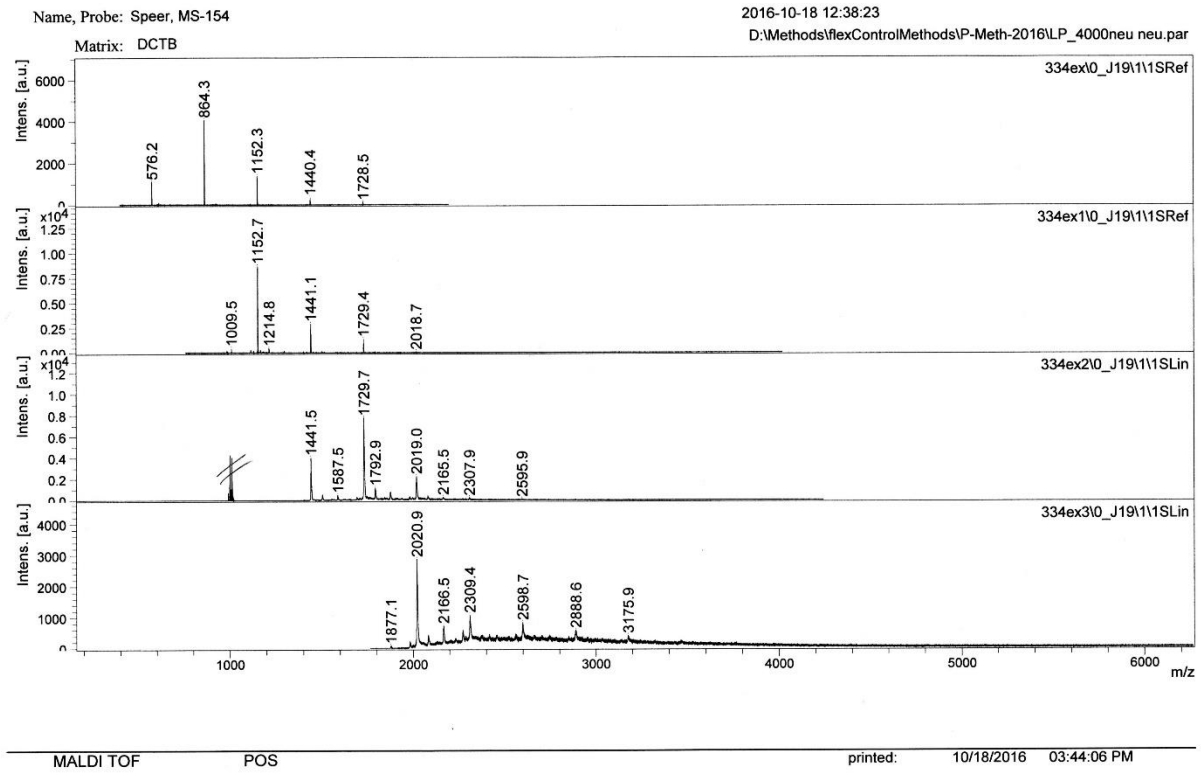

Figure S 31: MALDI-ToF spectra of polymer **P1**.

6 Thermal measurements

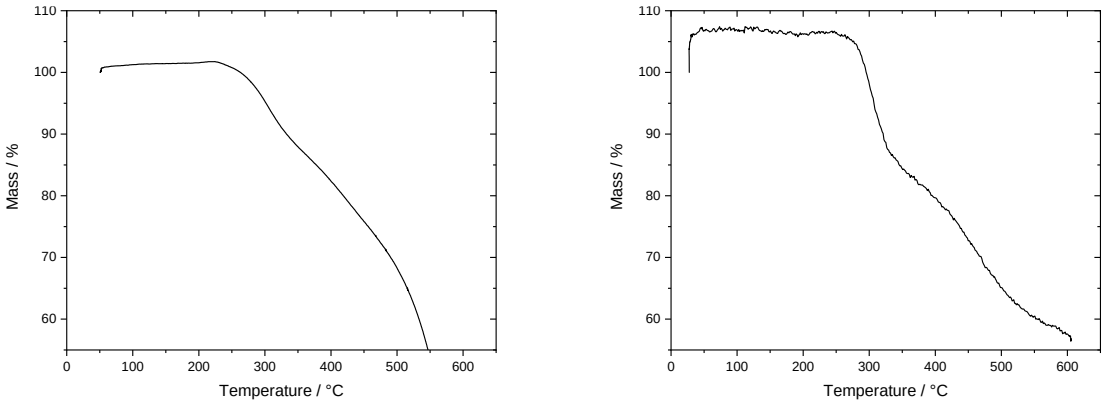

Figure S 32: TGA measurement of polymers **P1** (left) and **P3** (right) under air at a heating rate of 10 °C min^{-1} (Onsets decomposition:**P1** = 248 °C; **P3** = 262 °C, $TGA_{10\%}$: **P1** = 333 °C;**P3** = 321 °C).

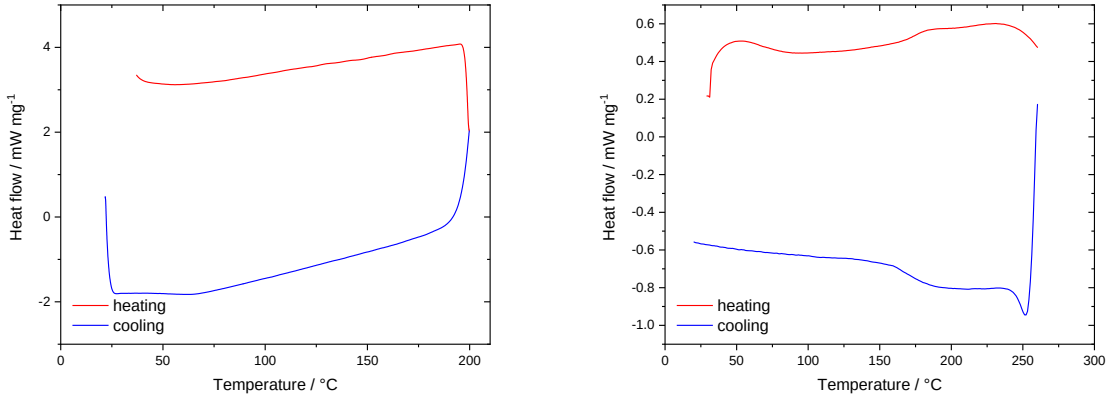

Figure S 33: DSC (heating: red line; cooling: blue line) of polymers **P1** (left) and **P3** (right) in N_2 atmosphere at a heating rate of 10 °C min^{-1}, no thermal events visible.

7 SEM/EDX mesurements

7.1 SEM measurements of polymer P2

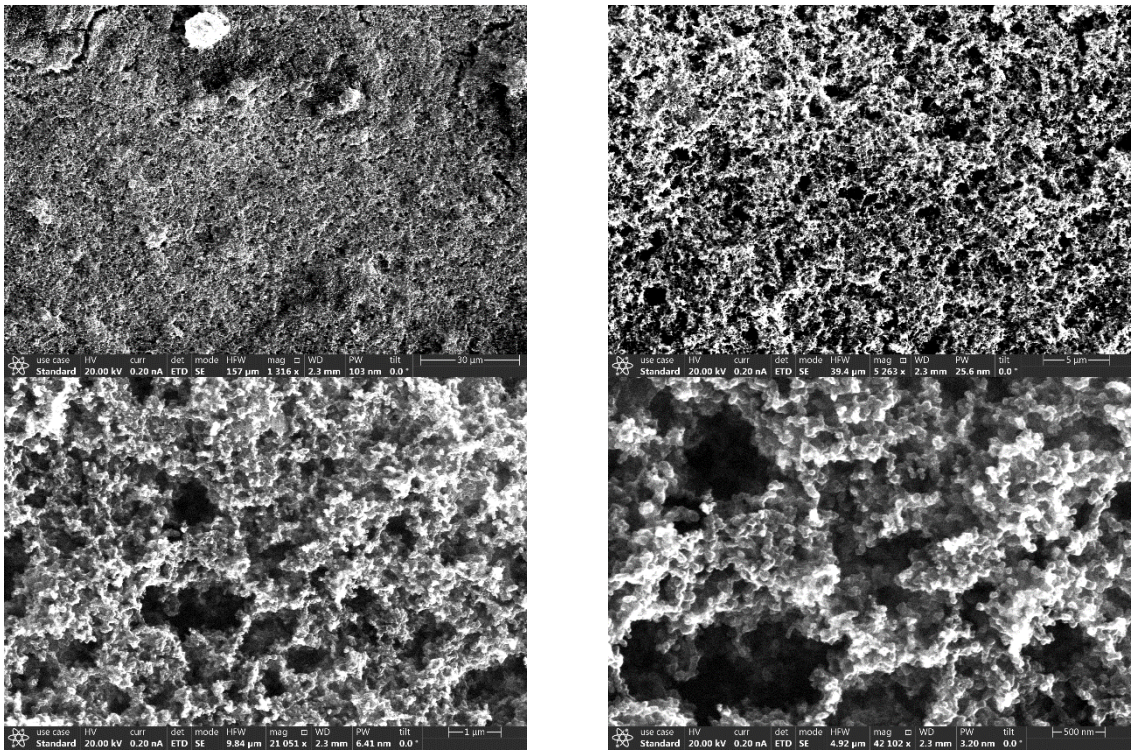

Figure S 34: SEM micrographs of a pristine **P2**-based composite electrode.

7.2 SEM/EDS measurements of polymer P3

7.2.1 Pristine Electrode

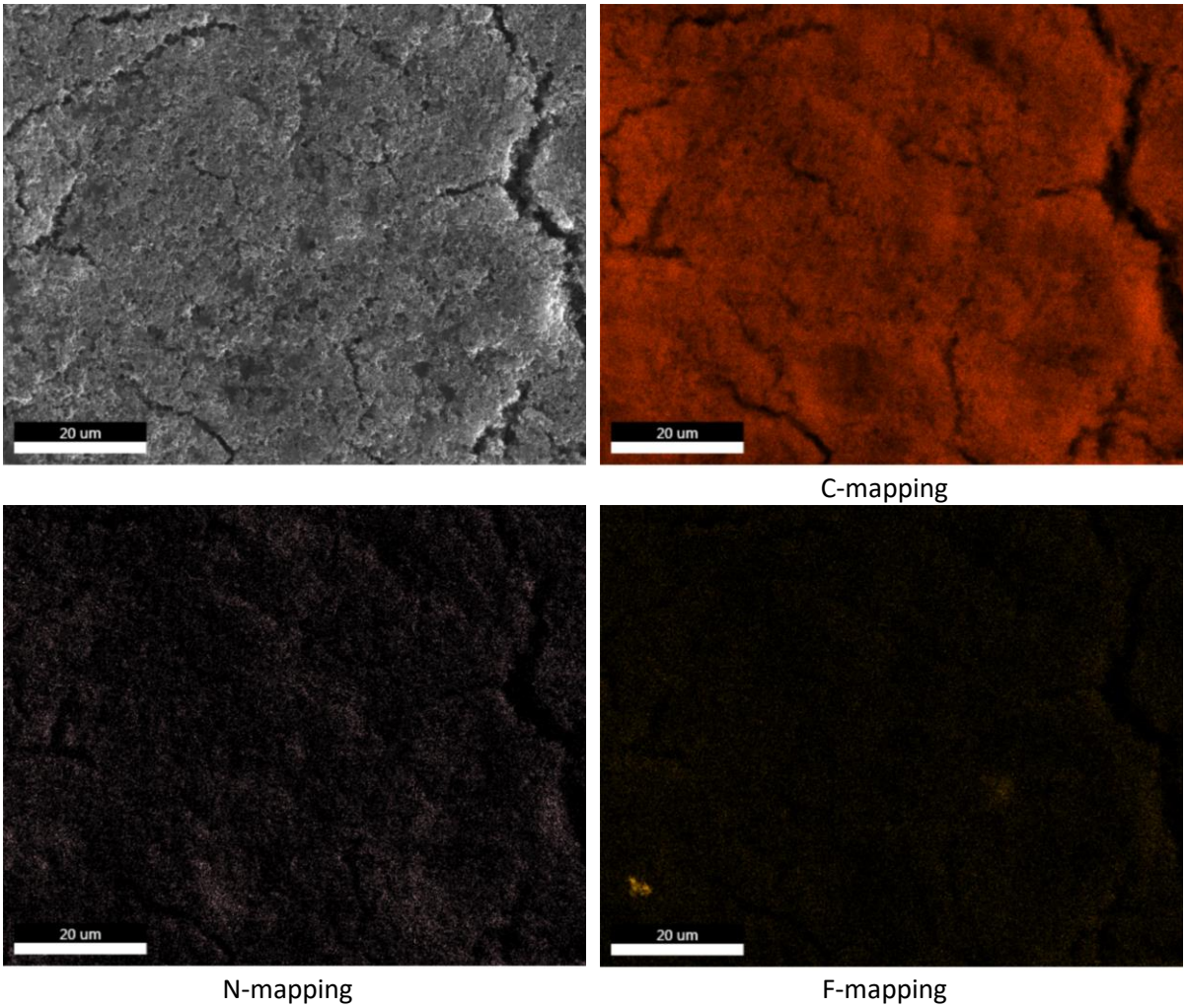

Figure S 35: EDS mappings of a pristine **P3**-based composite electrode.

7.2.1 Electrode after 200 cycles with EC/DMC: 1/1 + 1 M $LiPF_6$ as electrolyte

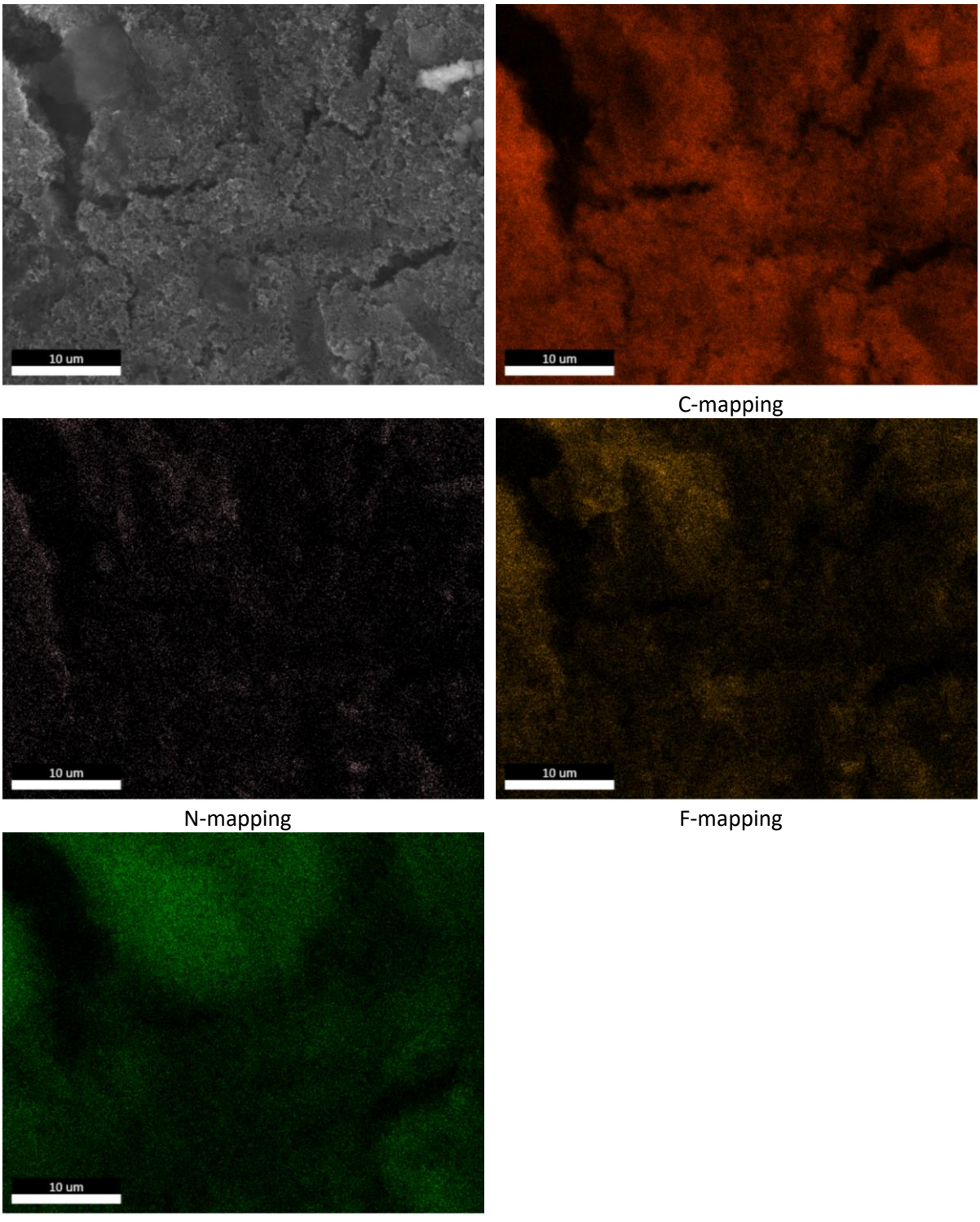

Figure S 36: EDS mappings of a **P3**-based composite electrode after 200 cycles with EC/DMC: 1/1 + 1 M $LiPF_6$ as electrolyte.

7.2.1 Electrode after 200 cycles with DOL/DME: 1/1 + 1M $LiClO_4$ as electrolyte

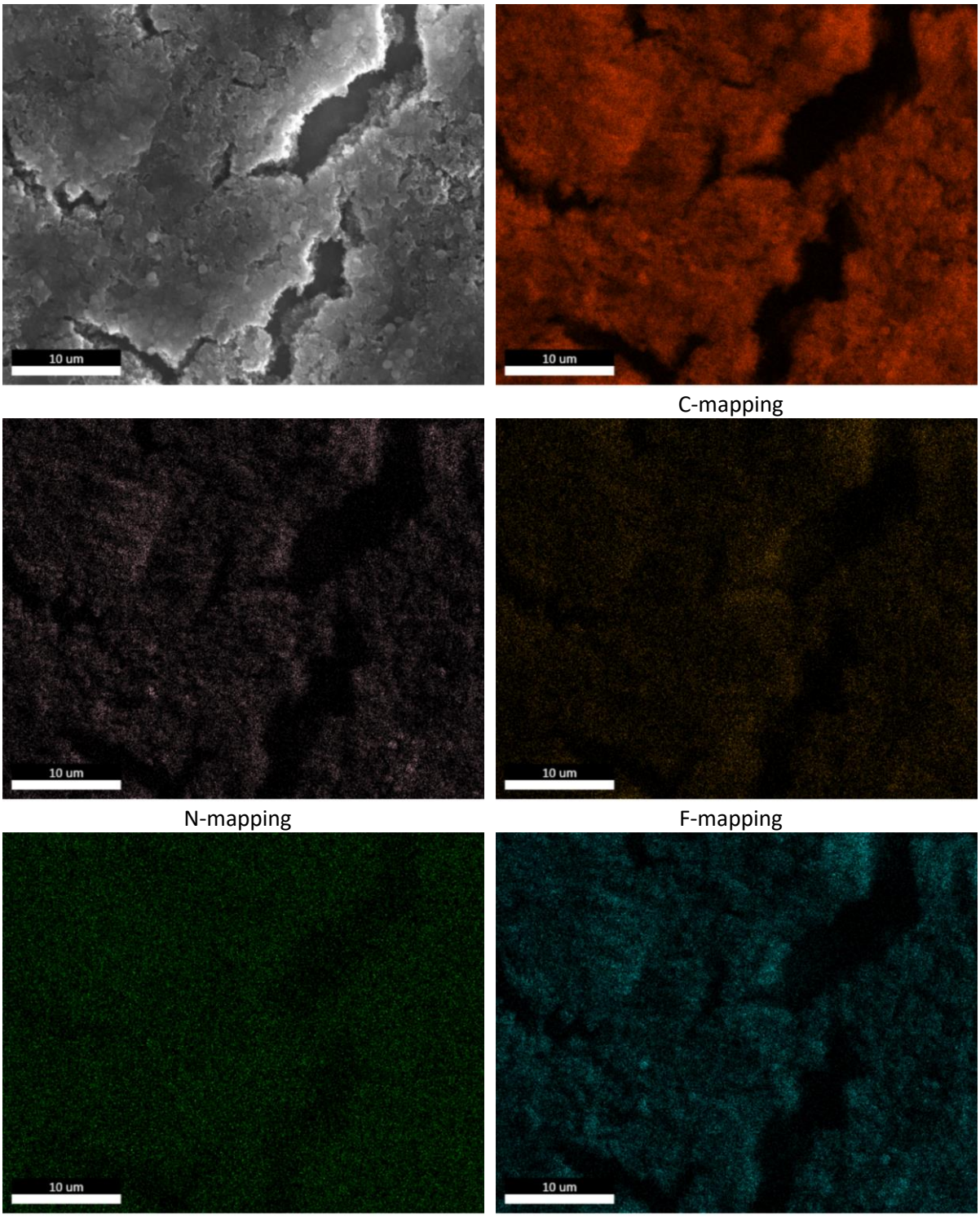

Figure S 37: EDS mappings of a **P3**-based composite electrode after 200 cycles with DOL/DME: 1/1 + 1 M $LiClO_4$ as electrolyte.

8 Crystal structure of model compound 2

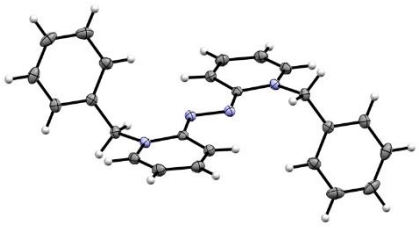

Experimental. Single red block-shaped crystals of model compound **2** were recrystallised from a mixture of dimethylformamide and methanol by solventlayering. The data for model compound **2** were collected from a shock-cooled single crystal at 100(2) K on a Bruker D8 VENTURE dual wavelength Mo/Cu three-circle diffractometer with a microfocus sealed X-ray tube using mirror optics as monochromator and a Bruker PHOTON III detector. The diffractometer was equipped with an Oxford Cryostream 800 low temperature device and used MoK_α radiation (λ = 0.71073 Å). All data were integrated with SAINT and a multi-scan absorption correction using SADABS was applied.[2,3] The structure were solved by direct methods using SHELXT and refined by full-matrix least-squares methods against F^2 by SHELXL-2018/3.[4,5] All non-hydrogen atoms were refined with anisotropic displacement parameters. The hydrogen atoms were refined isotropically on calculated positions using a riding model with their U_{iso} values constrained to 1.5 times the U_{eq} of their pivot atoms for terminal sp^3 carbon atoms and 1.2 times for all other carbon atoms. Crystallographic data (including structure factors) for the structures reported in this paper have been deposited with the Cambridge Crystallographic Data Centre.[6] CCDC 2001350 contain the supplementary crystallographic data for this paper. Copies of the data can be obtained free of charge from the Cambridge Crystallographic Data Centre via www.ccdc.cam.ac.uk/structures. This report and the CIF file were generated using FinalCif.[7]

Table S 3: Crystal data and structure refinement for model compound **2**.

CCDC number	2001350
Empirical formula	$C_{12}H_{11}N_2$
Formula weight	183.23
Temperature [K]	100(2)
Crystal system	monoclinic
Space group (number)	$P2_1/c$ (14)
a [Å]	9.4727(5)
b [Å]	10.4994(6)
c [Å]	9.5491(6)
α [Å]	90
β [Å]	101.527(3)
γ [Å]	90
Volume [Å^3]	930.58(9)
Z	4
ρ_{calc} [g/cm^3]	1.308
μ [mm^{-1}]	0.079
F(000)	388
Crystal size [mm^3]	0.1×0.1×0.1
Crystal colour	red
Crystal shape	block
Radiation	MoK_α (λ=0.71073 Å)
2Θ range [°]	5.83 to 50.27 (0.84 Å)
Index ranges	-10 ≤ h ≤ 11 -12 ≤ k ≤ 12 -11 ≤ l ≤ 11
Reflections collected	27035
Independent reflections	1641 R_{int} = 0.0288 R_{sigma} = 0.0103
Completeness to θ = 25.137°	98.5 %
Data / Restraints / Parameters	1641/0/127
Goodness-of-fit on F^2	1.443
Final *R* indexes [$I \geq 2\sigma(I)$]	R_1 = 0.0326 wR_2 = 0.1466
Final *R* indexes [all data]	R_1 = 0.0343 wR_2 = 0.1520
Largest peak/hole [eÅ^3]	0.21/-0.19

Table S 4: Atomic coordinates and U_{eq} [Å^2] for model compound **2**.

Atom	*x*	*y*	*z*	U_{eq}
N1	0.50318(8)	0.75158(8)	0.36352(9)	0.0160(3)
N2	0.47023(8)	0.95366(8)	0.44864(8)	0.0164(3)
C1	0.00624(11)	0.55919(11)	0.29593(13)	0.0283(4)
H1	-0.076104	0.512182	0.308247	0.034
C2	0.08585(11)	0.51967(11)	0.19778(12)	0.0255(3)
H2	0.056967	0.446301	0.141057	0.031
C3	0.20810(10)	0.58659(10)	0.18138(10)	0.0195(3)
H3	0.264033	0.557210	0.115667	0.023
C4	0.24885(10)	0.69612(9)	0.26054(10)	0.0162(3)
C5	0.38053(10)	0.77009(10)	0.24288(10)	0.0177(3)
H5A	0.409357	0.743118	0.153283	0.021
H5B	0.356218	0.861829	0.234251	0.021
C6	0.54908(10)	0.85097(9)	0.45954(10)	0.0149(3)
C7	0.16666(11)	0.73644(10)	0.35805(11)	0.0217(3)
H7	0.192900	0.811636	0.412362	0.026
C8	0.04669(12)	0.66740(12)	0.37631(12)	0.0286(4)
H8	-0.007765	0.694627	0.444253	0.034
C9	0.67999(10)	0.82566(10)	0.56276(11)	0.0179(3)
H9	0.722597	0.892224	0.624363	0.022
C10	0.74312(11)	0.71003(10)	0.57379(11)	0.0207(3)
H10	0.827821	0.695888	0.644228	0.025
C11	0.68420(11)	0.60894(10)	0.48102(11)	0.0215(3)
H11	0.725326	0.526104	0.491272	0.026
C12	0.56817(10)	0.63465(10)	0.37819(10)	0.0189(3)
H12	0.529906	0.568933	0.313227	0.023

U_{eq} is defined as 1/3 of the trace of the orthogonalized U_{ij} tensor.

Table S 5: Bond lengths and angles for model compound **2**.

Atom–Atom	Length [Å]
N1–C12	1.3679(13)
N1–C6	1.3999(12)
N1–C5	1.4764(11)
N2–C6	1.3038(13)
N2–N2$^{\#1}$	1.4163(15)
C1–C2	1.3790(18)
C1–C8	1.3818(17)
C1–H1	0.9500
C2–C3	1.3898(15)
C2–H2	0.9500
C3–C4	1.3879(14)
C3–H3	0.9500
C4–C7	1.3937(14)
C4–C5	1.5071(14)
C5–H5A	0.9900
C5–H5B	0.9900
C6–C9	1.4462(14)
C7–C8	1.3879(16)
C7–H7	0.9500
C8–H8	0.9500
C9–C10	1.3481(15)
C9–H9	0.9500
C10–C11	1.4232(15)
C10–H10	0.9500
C11–C12	1.3467(14)
C11–H11	0.9500
C12–H12	0.9500

Atom–Atom–Atom	Angle [°]
C12–N1–C6	121.83(8)
C12–N1–C5	117.77(8)
C6–N1–C5	120.39(8)
C6–N2–N2$^{\#1}$	111.74(9)
C2–C1–C8	119.75(10)
C2–C1–H1	120.1
C8–C1–H1	120.1
C1–C2–C3	120.37(10)
C1–C2–H2	119.8
C3–C2–H2	119.8
C4–C3–C2	120.32(10)

C4–C3–H3	119.8
C2–C3–H3	119.8
C3–C4–C7	118.94(9)
C3–C4–C5	120.82(9)
C7–C4–C5	120.24(9)
N1–C5–C4	112.63(8)
N1–C5–H5A	109.1
C4–C5–H5A	109.1
N1–C5–H5B	109.1
C4–C5–H5B	109.1
H5A–C5–H5B	107.8
N2–C6–N1	117.79(9)
N2–C6–C9	127.29(9)
N1–C6–C9	114.91(9)
C8–C7–C4	120.40(10)
C8–C7–H7	119.8
C4–C7–H7	119.8
C1–C8–C7	120.19(10)
C1–C8–H8	119.9
C7–C8–H8	119.9
C10–C9–C6	121.69(10)
C10–C9–H9	119.2
C6–C9–H9	119.2
C9–C10–C11	120.68(9)
C9–C10–H10	119.7
C11–C10–H10	119.7
C12–C11–C10	117.76(9)
C12–C11–H11	121.1
C10–C11–H11	121.1
C11–C12–N1	122.66(9)
C11–C12–H12	118.7
N1–C12–H12	118.7

Symmetry transformations used to generate equivalent atoms:
#1: 1-X, 2-Y, 1-Z;

9 DFT calculations on model compounds 2, $2^{\bullet+}$ and 2^{2+}

DFT calculations were performed with either the TURBOMOLE v7.3 program package.[8] The resolution-of-identity[9] (RI, RIJDX for SP) approximation for the Coulomb integrals was used in all DFT calculations employing matching auxiliary basis set def2-XVP/J.[10] Furthermore, the D3 dispersion correction scheme[11] with the Becke-Johnson damping function was applied.[12] Using the TURBOMOLE v7.3 program package, the geometries of all molecules were optimized without symmetry restrictions with the PBEh-3c[13]-D3/def2-mSVP composite scheme followed by harmonic vibrational frequency analysis to confirm minima as stationary points. This geometry was used as an input for further geometry optimizations. Following the structures were each optimized on the PBE0[14]-D3/def2-TZVP[15] level of theory. Single point energies were calculated using PW6B95[16] functional with the def2-TZVP basis set.[15]

9.1 COSMO calculations on model compound 2

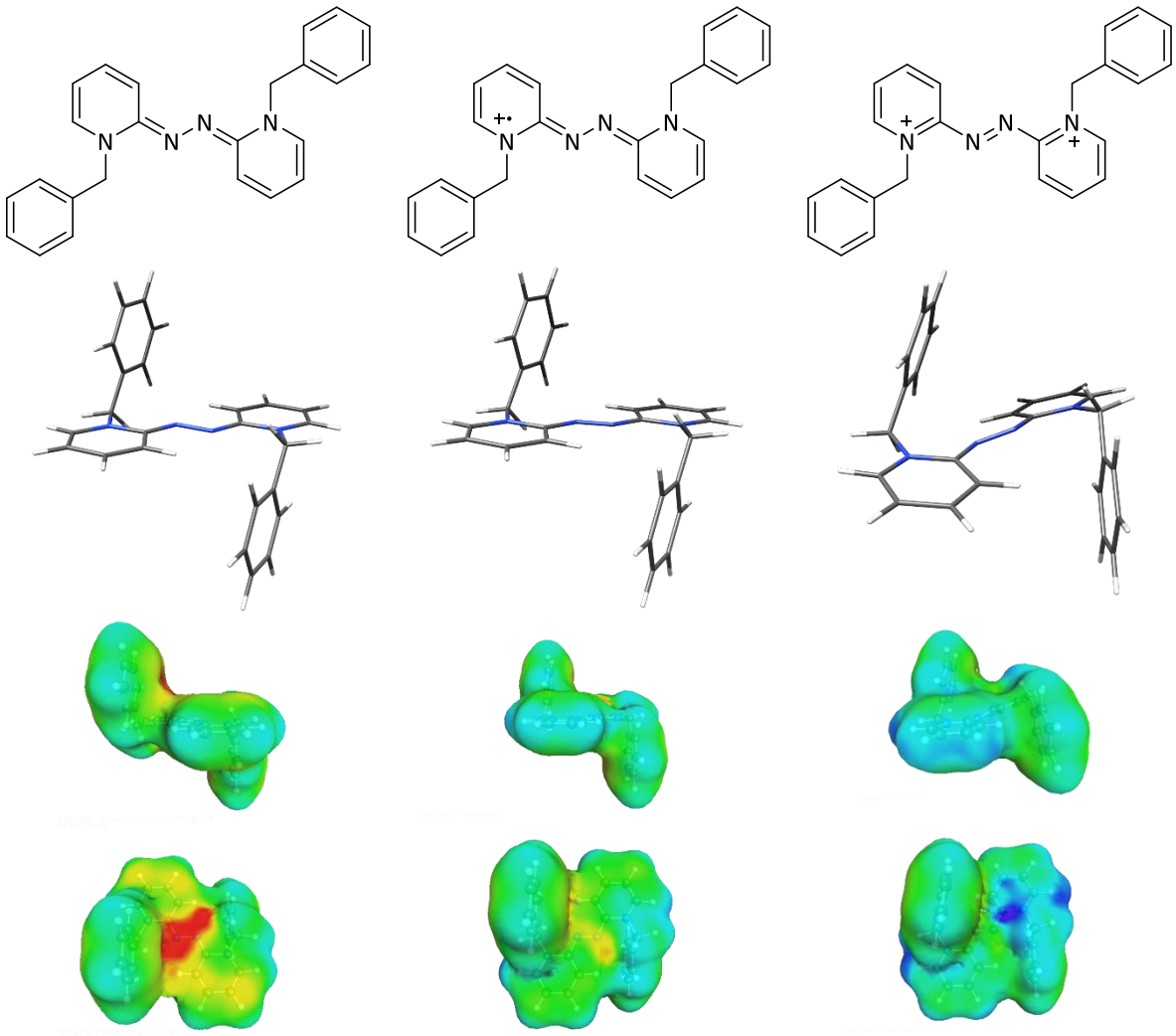

Figure S 38: Calculated structures of **2** in three oxidation states (PBE0-D3/def2-TZVP+COSMO(Acetonitrile)) and the resulting COSMO surface of the molecules (PW6B95-D3/def2-TZVP+COSMO(Acetonitrile). The COSMO surfaces of the molecules are color-coded based on the distribution of their surface properties: electron-rich regions (red), nonpolar (green) and electron-deficient regions (blue).

Table S 6: Energies obtained for **2**, **2**$^{\bullet+}$ and **2**$^{2+}$ after geometry optimization and calculation of the harmonic vibrational frequencies (PBE0-D3/def2-TZVP+COSMO(Acetonitrile)). Single point energies were calculated at the PW6B95-D3/def2-TZVP+COSMO(Acetonitrile) level of theory (all values are listed in hartrees).

	2	**2**$^{\bullet+}$	**2**$^{2+}$
E(PW6B95-D3) (E_h)[a]	−1148.7141131595	−1148.5611253292	−1148.3734907277
ZPE (E_h)[b]	0.41075394	0.41237195	0.41921902
Total enthalpy (E_h)[b]	−1145.45518049	−1145.30815012	−1145.12073387
Final entropy term (E_h)[b]	0.07345645	0.06779460	0. 0.07003855
Gibbs free energy (E_h)[b]	−1145.52863694	−1145.37594472	−1145.19077242
Gibbs free energy minus the electronic energy (E_h)[b]	0.36125823	0.36560681	0.36702439

[a] PW6B95-D3/def2-TZVP, [b] PBE0-D3/def2-TZVP.

Table S 7: Frontier molecular orbital energies (PW6B95-D3/def2-TZVP+COSMO(Acetonitrile)) of **2** (uncharged), **2**$^{\bullet+}$ (radical cation), and **2**$^{2+}$ (dication) (all values are listed in eV).

Molecular Orbital	**0**	**+1$_\alpha$ / +1$_\beta$**	**+2**
LUMO+1	−0.84	−1.73/ −1.57	−2.59
LUMO	−0.85	−1.78/ −1.63	−4.38
HOMO	−4.65	−5.65 / −3.44 (unoccupied)	−7.75
HOMO−1	−6.19	−7.23/ −7.10	−7.80
GAP$_{HOMO/LUMO}$	**3.80**	**2.20 (spin flip)**	**3.36**

Table S 8: Free energies of the oxidation potentials calculated from the energies listed in **Table S 7** (PW6B95-D3/def2-TZVP//PBE0-D3/def2-TZVP+COSMO(Acetonitrile)).

Oxidation process of	**ΔG_{ox} [hartrees]**[a]	**ΔG_{ox} [kcal mol^{-1}]**[a]	***E* [V]**[b]
tmp2 → **tmp2**$^{\bullet+}$ + e$^-$	0.15734	98.73	−4.28
tmp2$^{\bullet+}$ → **tmp2**$^{2+}$ + e$^-$	0.18905	118.6	−5.14

[a] $\Delta G_{ox} = E_{tot}$ PW6B95-D3/def2-TZVP+ Gibbs free energy minus the electronic energy (PBE0-D3/def2-TZVP+), [b] V for one electron transfer.

9.2 Nucleus-independent chemical shift value

Nucleus-independent chemical shift (NICS) values were calculated using the Gaussian 09 program package applying the standard Gauge-Including Atomic Orbitals (GIAO) method on the B3LYP/6-31G*level of theory.

Table S 9: Calculated nucleus independent chemical shift values of **2**, $\mathbf{2}^{\bullet+}$ and $\mathbf{2}^{2+}$ (B3LYP/6-31G*).

Position	2	2^{+}	2^{2+}
1	−2.00	−6.53	−9.60
2	−1.57	−6.11	−9.09
3	−2.00	−6.19	−9.47
4	−1.58	−6.57	−9.39

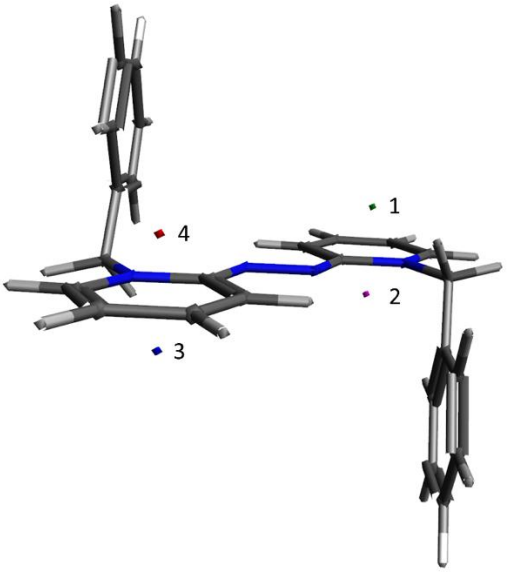

Figure S 39: Representative positions of the dummy atoms for the $NICS_1$ (iso) calculations of **2**. Each dummy atom is positioned 1 Å above the respective ring plane.

9.3 Cartesian coordinates of calculated structures

Table S 10: Coordinates of the calculated structure of **2** (PBE0/def2- TZVP+COSMO(Acetonitrile)).

	x	y	z
N	0.8492703	0.3007603	2.3245288
C	1.2074369	-0.1729575	1.0607163
C	2.5315932	-0.7210113	0.9482525
C	3.3623276	-0.7736765	2.0178635
C	2.9439496	-0.2820867	3.2834299
C	1.6961759	0.2413184	3.3803254
N	0.3109156	-0.0675605	0.1270362
N	0.7224190	-0.5613476	-1.0871771
C	-0.1737459	-0.4549690	-2.0211250
C	-1.4971079	0.0951577	-1.9091850
C	-2.3274520	0.1488964	-2.9790529
C	-1.9094686	-0.3436823	-4.2443577
C	-0.6625226	-0.8691497	-4.3407030
N	0.1839751	-0.9296927	-3.2846367
C	-0.4774920	0.8614634	2.4891148
C	-1.5796548	-0.1637531	2.4430166
C	1.5095410	-1.4935186	-3.4485019
C	2.6140318	-0.4708346	-3.4026208
C	2.4460265	0.7990610	-3.9426032
C	3.4887101	1.7151596	-3.9264975
C	4.7152349	1.3677356	-3.3757586
C	4.8903214	0.0983756	-2.8398728
C	3.8441234	-0.8123409	-2.8523585
C	-2.8116565	0.1764069	1.8961887
C	-3.8558169	-0.7366334	1.8834918
C	-3.6767980	-2.0069712	2.4157557
C	-2.4483943	-2.3529908	2.9631616
C	-1.4077368	-1.4345959	2.9794679
H	2.8251433	-1.0734041	-0.0298140
H	4.3573590	-1.1912004	1.9078521
H	3.5875725	-0.3085258	4.1510460
H	1.3024430	0.6412430	4.3056684
H	-1.7902755	0.4483636	-0.9312979
H	-3.3218137	0.5681298	-2.8694324
H	-2.5527669	-0.3164433	-5.1121983
H	-0.2692242	-1.2700899	-5.2657845
H	-0.4879797	1.3774946	3.4516102
H	-0.6415750	1.6007638	1.7033842
H	1.6716339	-2.2328143	-2.6623196
H	1.5190890	-2.0100229	-4.4107467
H	1.4897080	1.0823486	-4.3692631
H	3.3419740	2.7041558	-4.3460330
H	5.5294952	2.0835885	-3.3606594
H	5.8420673	-0.1799218	-2.4012860
H	3.9792707	-1.7980110	-2.4189122
H	-2.9499382	1.1628701	1.4655213
H	-4.8090772	-0.4593447	1.4475620
H	-4.4894770	-2.7246144	2.4004496
H	-2.2985654	-3.3426976	3.3799207
H	-0.4499292	-1.7168206	3.4034733

Table S 11: Coordinates of the calculated structure of **2**$^{\bullet+}$ (PBE0-D3/def2-TZVP+COSMO(Acetonitrile)).

	x	y	z
N	0.9183647	0.3024516	2.2753592
C	1.2820865	-0.2005008	1.0539407
C	2.5571173	-0.7822167	0.9291408
C	3.3983640	-0.8412954	2.0077124
C	2.9902141	-0.3191086	3.2414364
C	1.7477484	0.2434661	3.3338798
N	0.3624817	-0.0619193	0.0844822
N	0.7027672	-0.6299855	-1.0459651
C	-0.2238045	-0.5029537	-2.0104606
C	-1.5144851	0.0397134	-1.8714337
C	-2.3641412	0.0847478	-2.9441404
C	-1.9489751	-0.4128871	-4.1856516
C	-0.6905329	-0.9361166	-4.2921023
N	0.1474934	-0.9803032	-3.2396867
C	-0.4114319	0.8931317	2.4375278
C	-1.5196746	-0.1209473	2.3696595
C	1.4964794	-1.5214998	-3.4176235
C	2.5665394	-0.4675880	-3.3425279
C	2.3710221	0.8041919	-3.8684634
C	3.3859286	1.7490064	-3.8135747
C	4.6084569	1.4278140	-3.2393120
C	4.8101360	0.1561441	-2.7193994
C	3.7924484	-0.7847658	-2.7689379
C	-2.7379187	0.2450061	1.8084502
C	-3.7914283	-0.6559976	1.7657267
C	-3.6340463	-1.9361861	2.2801613
C	-2.4195056	-2.3058693	2.8419079

C	-1.3683951	-1.4009157	2.8900906	H	1.5037311	-2.0101768	-4.3925510
H	2.8371315	-1.1619989	-0.0421998	H	1.4203801	1.0692260	-4.3188395
H	4.3792413	-1.2896319	1.9058481	H	3.2199398	2.7392103	-4.2221073
H	3.6275390	-0.3466015	4.1137447	H	5.4003819	2.1668465	-3.1942950
H	1.3644224	0.6661809	4.2519830	H	5.7597032	-0.1016463	-2.2645603
H	-1.8000126	0.3991259	-0.8937860	H	3.9481713	-1.7740346	-2.3513617
H	-3.3573627	0.5022839	-2.8315148	H	-2.8588811	1.2408817	1.3950717
H	-2.5928602	-0.3962186	-5.0533978	H	-4.7345802	-0.3603404	1.3206642
H	-0.3002777	-1.3363265	-5.2172742	H	-4.4541648	-2.6440742	2.2402350
H	-0.4068451	1.3947061	3.4059385	H	-2.2877235	-3.3031520	3.2456412
H	-0.5460213	1.6468061	1.6631141	H	-0.4243604	-1.7047239	3.3297670
H	1.6624789	-2.2793483	-2.6536766				

Table S 12: Coordinates of the calculated structure of **2**$^{2+}$ (PBE0-D3/def2-TZVP+COSMO(Acetonitrile)).

	x	**y**	**z**				
N	1.2195468	0.2268058	2.0535770	H	3.8614544	-0.5320153	3.9334281
C	1.5090642	-0.4737375	0.9305457	H	1.7399688	0.7634542	3.9683665
C	2.6652529	-1.2192355	0.8451957	H	-1.8632692	-0.4756094	-0.7146592
C	3.5341080	-1.2487864	1.9238646	H	-3.5555039	-0.4679330	-2.5650926
C	3.2170958	-0.5347618	3.0652764	H	-2.7835307	-0.9791250	-4.8919160
C	2.0450101	0.1936965	3.1023478	H	-0.3681892	-1.4350755	-5.2760757
N	0.5607856	-0.3206123	-0.0840821	H	0.0362297	1.5647202	3.0770166
N	0.7322440	-1.0671931	-1.0591989	H	-0.0114081	1.7377783	1.3213888
C	-0.2664339	-0.9480960	-2.0286869	H	1.8377970	-2.3885075	-3.0294239
C	-1.5865192	-0.6731088	-1.7419378	H	1.6150846	-1.6928186	-4.6389240
C	-2.5141267	-0.6812153	-2.7705536	H	1.1083406	1.1884237	-3.9611520
C	-2.0947362	-0.9637766	-4.0589845	H	2.5542269	3.0546544	-3.2799049
C	-0.7611450	-1.2283349	-4.2905982	H	4.6911952	2.6148365	-2.1093357
N	0.1254148	-1.2313193	-3.2905921	H	5.3762362	0.2825291	-1.6329693
C	-0.0231999	1.0164312	2.1374258	H	3.9176511	-1.5928366	-2.3027586
C	-1.2637736	0.1709909	2.0745813	H	-2.4199205	1.7869630	1.2623557
C	1.5527971	-1.4873766	-3.5711207	H	-4.5088041	0.4810749	1.1486668
C	2.4194427	-0.3273877	-3.1726022	H	-4.5308138	-1.8915567	1.8650496
C	2.0439145	0.9826377	-3.4520811	H	-2.4545461	-2.9315024	2.7265300
C	2.8579886	2.0364594	-3.0669017	H	-0.3836929	-1.6284982	2.8700880
C	4.0579043	1.7891384	-2.4117489				
C	4.4424234	0.4828237	-2.1447972				
C	3.6236901	-0.5716296	-2.5206436				
C	-2.4328990	0.7550826	1.5963041				
C	-3.6053436	0.0185113	1.5286265				
C	-3.6174700	-1.3118030	1.9301427				
C	-2.4543846	-1.8953244	2.4100989				
C	-1.2820296	-1.1551302	2.4891261				
H	2.8634773	-1.7626087	-0.0671477				
H	4.4467349	-1.8284858	1.8705263				

10 References

[1] G. Socrates, *Infrared and Raman Characteristic Group Frequencies, Tables and Charts, Third Edition*, John Wiley & Sons, Chichester, 2001.

[2] Bruker, *SAINT*, *V8.40A*, Bruker AXS Inc., Madison, Wisconsin, USA.

[3] Bruker, *SADABS*, *2016/2*, Bruker AXS Inc., Madison, Wisconsin, USA.

[4] G. M. Sheldrick, *Acta Cryst.* **2015**, *A71*, 3–8.

[5] G. M. Sheldrick, *Acta Cryst.* **2015**, *C71*, 3–8.

[6] C. R. Groom, I. J. Bruno, M. P. Lightfoot, S. C. Ward, *Acta Cryst.* **2016**, *B72*, 171–179.

[7] D. Kratzert, *FinalCif*, *V58*, https://www.xs3.uni-freiburg.de/research/finalcif

[8] TURBOMOLE V6.2 2010, 1989-2007 Forschungszentrum Karlsruhe GmbH, since 2007; available from TURBOMOLE GmbH, http://www.turbomole.com.

[9] K. Eichkorn, O. Treutler, H. Öhm, M. Häser, R. Ahlrichs, *Chem. Phys. Lett.* **1995**, *240*, 283–290.

[10] F. Weigend, *Phys. Chem. Chem. Phys.* **2006**, *8*, 1057.

[11] S. Grimme, J. Antony, S. Ehrlich, H. Krieg, *J. Chem. Phys.* **2010**, *132*, 154104.

[12] E. R. Johnson, A. D. Becke, *J. Chem. Phys.* **2006**, *124*, 174104.

[13] S. Grimme, J. G. Brandenburg, C. Bannwarth, A. Hansen, *J. Chem. Phys.* **2015**, *143*, 054107.

[14] C. Adamo, V. Barone, *J. Chem. Phys.* **1999**, *110*, 6158–6170.

[15] A. Schäfer, C. Huber, R. Ahlrichs, *J. Chem. Phys.* **1994**, *100*, 5829–5835.

[16] Y. Zhao, D. G. Truhlar, *J. Phys. Chem. A* **2005**, *109*, 5656–5667.